




Article

Reproductive Structures of Female *Phytoseiulus persimilis* (Acari: Phytoseiidae) and the Development of Egg and Embryo in the Body

Binting Huang ^{1,2,†} , Mingxia Li ^{2,†}, Xiaohuan Jiang ², Bo Zhang ^{2,3} , Yong Huang ^{1,*} and Xuenong Xu ^{2,3,*} ¹ Institute of Plant Protection, Anhui Agricultural University, Hefei 230036, China; bintingh@126.com² State Key Laboratory for Biology of Plant Diseases and Insect Pests, Institute of Plant Protection, Chinese Academy of Agricultural Sciences, Beijing 100193, China; lmx2396136022@163.com (M.L.); mxczjh@126.com (X.J.); zhangbo05@caas.cn (B.Z.)³ Key Laboratory of Natural Enemies Insects, Ministry of Agriculture and Rural Affairs, Beijing 100193, China

* Correspondence: yongh2017@ahau.edu.cn (Y.H.); xuxuenong@caas.cn (X.X.)

† These authors contributed equally to this work.

Abstract: The *Phytoseiulus persimilis* specialized in preying on Tetranychus species, with particularly strong predation capability against *Tetranychus urticae*. To investigate the morphology of female reproductive structures and effects of different gravid times on structures of oocytes and embryos in *Phytoseiulus persimilis*, we employed paraffin sectioning, transmission electron microscopy (TEM), and scanning electron microscopy (SEM) on the model species of predatory mite *Phytoseiulus persimilis*. The female adult possessed several reproductive organs, including paired solenostomes, major ducts, embolus, calyces, and vesicles within the sperm-access system, as well as lyrate organ and the ovary. Furthermore, the reproductive system also encompassed the uterus, vagina, and genital pore, which were involved in egg development and expulsion. The solenostomes were situated between the third and fourth legs, and they were scarcely discernible in virgin, but they became apparent during mating. The occurrence of mating significantly influenced the nucleus of lyrate organ. In virgin, the nucleus exhibited underdeveloped morphology, whereas in mated individuals, it was well-formed. However, the duration of mating did not impact its development. The cellular structure of the ovary was solely associated with the stage of the surrounding oocyte and was not directly linked to mating occurrences. The uterus was barely visible outside of mating periods but became observable 12 h after mating when eggs were present within the body. At this point, it opened in preparation for egg laying when both the vagina and reproductive opening were open. Positioned in front of the vesicle but behind the ovary was the lyrate organ, with its lower part housing the uterus. The vagina was connected to the genital pore. No significant difference was observed in oocyte morphology between the virgin ovaries and the mated. Oocyte development occurred through four stages: during stage I (4–9 h after mating), yolk accumulation took place; stage II (10 h after mating) involved egg relocation; stage III (12–13 h after mating) was marked by eggshell formation; finally, at stage IV (14–16 h after mating), embryonic development commenced, leading to egg deposition. The fusion of sperm and egg occurred approximately 9–10 h after mating. These findings established a solid foundation for investigating the Phytoseiid reproductive mechanisms.

Keywords: predatory mite; female reproductive structures; egg formation; electron microscopes



Citation: Huang, B.; Li, M.; Jiang, X.; Zhang, B.; Huang, Y.; Xu, X. Reproductive Structures of Female *Phytoseiulus persimilis* (Acari: Phytoseiidae) and the Development of Egg and Embryo in the Body. *Agriculture* **2024**, *14*, 1647. <https://doi.org/10.3390/agriculture14091647>

Academic Editor: Marco Scortichini

Received: 22 August 2024

Revised: 13 September 2024

Accepted: 15 September 2024

Published: 20 September 2024



Copyright: © 2024 by the authors. Licensee MDPI, Basel, Switzerland. This article is an open access article distributed under the terms and conditions of the Creative Commons Attribution (CC BY) license (<https://creativecommons.org/licenses/by/4.0/>).

1. Introduction

Phytoseiulus persimilis, a pivotal predator of spider mites, had served as an efficacious biocontrol agent for nearly half a century [1]. Although extensive research has been conducted on its biology and ecology [2–4], investigations into the ultrastructure of its reproductive system remain limited and outdated, primarily attributed to the works of Alberti and Nuzzaci [5,6]. The female reproductive system in Phytoseiidae encompassed

paired gonads, a uterus, and a vaginal duct [7]. The gonads consisted of ovaries where germ cells underwent development alongside a lyrate organ comprising supportive and nutritive tissues [7]. Unlike other Dermanyssina species that employ follicular sperm-entry systems, Phytoseiidae exhibited a distinct sperm-access apparatus involving paired solenostomes, major and minor ducts, a plug, calyx structures, and vesicles [8].

After mating, oocytes underwent four distinct stages characterized by changes in structure and organelle abundance, leading to progressive maturation. Notably, during stage III, the cell membrane exhibited yolk droplets and small protrusions. In stage IV oocytes, peripheral cytoplasm revealed numerous yolk granules and large vesicles, indicating further maturation. Additionally, potential sperm cells might also be present in the ovaries [7].

Research on Phytoseiidae has investigated the occurrence of haploid males and diploid females [9–12]. Toyoshima's study focused on egg development in female *Ph. persimilis*, revealing that two pronuclei appear in the egg 9 h after mating, fused by 12.7 h, and the pronuclei of the second egg began merging by 13.5 h [13]. However, existing research primarily examined the reproductive aspects of female Phytoseiidae with limited emphasis on *Ph. persimilis*, specifically. Furthermore, the available literature predominantly described internal reproductive structures without comprehensive coverage of overall morphology or the effects of different gravid durations on structures or spatial relationships between structures. The scarcity of studies investigating processes related to egg formation and sperm–egg fusion within eggs resulted in insufficient evidence for accurately estimating timing during egg and embryo development stages. By employing three imaging techniques to explore structural morphology and dissecting female mites at different mating times to observe egg formation, it is possible to obtain a more precise estimation of sperm–egg fusion and embryo development timelines. Our study aimed to provide insights into haploid males within the Phytoseiidae family while advancing our understanding of morphological structures, potentially enhancing the efficacy of predatory mites in biological control.

2. Materials and Methods

2.1. Rearing Conditions for *Phytoseiulus persimilis*

The *Ph. persimilis* colony has been reared on *Tetranychus urticae* for more than 10 years in the Lab of Predatory Mites, Institute of Plant Protection, Chinese Academy of Agricultural Sciences, Beijing, China. The *T. urticae* colony was maintained on bean seedlings [14]. We planted 23 bean seedlings (*Phaseolus vulgaris* L.) in a box (35 × 22.5 cm) and reared spider mites on the bean leaves 1 week later. The rearing conditions are 25 ± 1 °C, 70 ± 5% RH, and L:D = 16:8 h.

2.2. Sample Collection

A batch of newly laid eggs was obtained from a laboratory-reared population of *Ph. persimilis*. The eggs were individually transferred to small breeding chambers and reared until adulthood. Female and male adult mites were then paired for mating. After mating, female mites were collected at 17 time points ranging from 0 to 16 h post-mating, with 20 mites collected at each time point. These mites were placed in a 4% formaldehyde fixative solution (Shanghai Macklin Biochemical Technology Co., Ltd., Shanghai, China) for paraffin section sample preparation (HE) [15].

Additionally, 100 female mites were collected immediately after mating and soaked in lactic acid (Beijing Hwrk Chemical Technology Co., Ltd., Beijing, China) for 24 h for scanning electron microscope (SEM) [16]. Female mites that were either unmated or collected at 4, 10, and 12 h post-mating, with approximately 50 mites at each time point, were placed in fixative solution for transmission electron microscope (TEM) [17].

2.3. Paraffin Section Sample Preparation (HE Staining) [15]

- Tissue Fixation: Fixed the mite samples in 4% formaldehyde solution for 24 h.

- Ethanol Dehydration: Dehydrated the mite tissue stepwise by soaking it in ethanol solutions (Sinopharm Chemical Reagent Co., Ltd., Shanghai, China) of increasing concentrations (70%, 80%, 90%, 95%, 95%, 100%, and 100%) for 40 min each.
- Tissue Clearing: Immersed the mite tissue in three glass jars filled with xylene (Beijing Chemical Works, Beijing, China), soaking in each jar for 1 h.
- Wax Impregnation: Immersed the mite tissue in three glass jars filled with paraffin (Beijing Rhawn Chemical Reagent, Beijing, China), soaking in each jar for 1 h.
- Embedding: Poured melted paraffin into a metal mold, then placed the wax-impregnated tissue flat at the bottom of the mold, ensuring the cutting surface is facing downward. After the paraffin solidifies, removed the embedding mold. Once the paraffin was completely cooled and hardened, trimmed the wax block, leaving an appropriate amount of paraffin around the tissue for sectioning.
- Sectioning: Fixed the pre-cooled wax block onto a microtome (Zhejiang Jinhua Kedee Instrumental Equipment Co., Ltd., Jinhua, China). Aligned the cutting surface of the wax block parallel to the blade. Rotated the wheel to advance the block, adjusting the section thickness to 5 μm , and cut uniform sections, which were then placed into a slide flotation bath with water at about 45 °C. Spread the section flat on the water surface before mounting.
- Mounting Sections: Picked up the section on the slide and air-dried slightly. The sections were placed in a 60 °C oven (Shanghai Jinghong Instrument Equipment Co., Ltd., Shanghai, China) for 3 h.
- Deparaffinization: Gradually deparaffinized the sections by soaking them in the following solutions in sequence for the indicated times: xylene for 5 min, xylene for 5 min, absolute ethanol for 5 min, absolute ethanol for 5 min, 95% ethanol for 5 min, and 75% ethanol for 5 min, followed by washing the sections in water.
- HE Staining: Immersed the deparaffinized sections in hematoxylin-staining solution (Sinopharm Chemical Reagent Co., Ltd., Shanghai, China) for 10 min, then rinsed them with tap water. Differentiated the staining by immersing the sections in 1% hydrochloric acid alcohol (Beyotime Biotechnology, Shanghai, China) for a few seconds to remove excess hematoxylin from the cytoplasm. Rinsed again with tap water. After rinsing, immersed the sections in a bluing solution for 5–10 min. After bluing, immersed the sections in eosin-staining solution (Sinopharm Chemical Reagent Co., Ltd., Shanghai, China) for 3 min, and, finally, rinsed with tap water to complete the staining.
- Dehydration and Mounting: Cleared the stained sections by immersing them in the following solutions in sequence: 75% ethanol for 1 min, 95% ethanol for 1 min, absolute ethanol for 5 min, absolute ethanol for 5 min, xylene for 5 min, and xylene for 5 min. After clearing, mounted the sections with neutral resin (Shanghai Macklin Biochemical Technology Co., Ltd., Shanghai, China).

2.4. Sample Preparation for Scanning Electron Microscopy (SEM) [16]

- Tissue Fixation: Fixed the mites in 2.5% glutaraldehyde solution (Sigma-Aldrich, Shanghai branch, Shanghai, China) at 4 °C for 12 h.
- Buffer Washing: Washed the samples three times with 0.1 M phosphate-buffered saline (pH 7.4) (Sinopharm Chemical Reagent Co., Ltd., Shanghai, China), with each wash lasting 10 min.
- Gradient Dehydration: Dehydrated the samples sequentially using ethanol solutions of increasing concentrations (50%, 70%, 80%, 90%, 95%, and 100%) for 10 min each.
- Drying: Dried the samples using a critical point dryer (Leica EM, CPD300, Berlin, Germany).
- Removing the Dorsal Plate: Used a #0 insect needle under a microscope to remove the dorsal plate of the female mites (Chongqing Optec Instrument Co., Ltd., Chongqing, China).
- Mounting: Mounted the samples in an appropriate orientation on a black double-sided conductive adhesive, ensuring that the dorsal side of the mite is facing up.

- **Gold Coating and Observation:** Placed the prepared samples in a small ion sputter coater (Leica EM, ACE600, Germany) and applied a 4 nm layer of platinum. After coating, observed the samples under a scanning electron microscope (Hitachi, Regulus 8100, Tokyo, Japan) at 3 kV voltage.

2.5. Sample Preparation for Transmission Electron Microscopy (TEM) [17]

- **Tissue Fixation:** Prepared a fixative solution by adding Tween 100 (600 µL per 1 L) (Sinopharm Chemical Reagent Co., Ltd., China) and sodium chloride (0.9 g per 1 L) (Sinopharm Chemical Reagent Co., Ltd., China) to a 3.5% glutaraldehyde solution with pH 7.2. Placed 5 mL of this fixative solution in a centrifuge tube and fixed the mite samples for 48 h.
- **Washing:** Washed the samples with 0.2 M phosphate buffer, changing the buffer every 15 min, and repeated the wash 15 times.
- **Osmium Tetroxide Fixation:** Fixed the tissue with 1% osmium tetroxide (Structure Probe, Inc., West Chester, PA, USA) for 2 h.
- **Washing:** Performed continuous washes with 0.2 M phosphate buffer, 3–4 times.
- **Dehydration:** Dehydrated the samples sequentially in ethanol solutions of increasing concentrations (30%, 50%, 60%, 70%, 80%, 90%, 95%, and 100%), with each step lasting 5–8 min.
- **Ethanol-Acetone Substitution:** Substituted ethanol with acetone (Sinopharm Chemical Reagent Co., Ltd., China), 4–5 times, each for 15 min. Retained a small amount of acetone solution.
- **Resin Embedding:** Added pure resin to the acetone, mixed thoroughly with a toothpick, and soaked the samples for 12 h.
- **Polymerization:** Placed the resin-embedded samples in an oven at 35 °C and baked for 2–3 weeks.
- **Sectioning:** Cut the samples into thin sections of approximately 80–100 nm using a microtome (Leica, EM UC7, Tokyo, Japan).
- **Staining:** Stained the sections with uranyl acetate (Sigma-Aldrich, Shanghai branch, China) and lead citrate (Sigma-Aldrich, Shanghai branch, China) for about 1 h.

3. Results

3.1. Female Reproductive Structures

3.1.1. Solenostome, Major Duct, Embolus, Calyx, and Vesicle

The female possessed a pair of solenostomes located between the third and fourth pairs of legs on each side of the body. These solenostomes facilitated the insertion of the male mites' spermatodactyl during mating for sperm transfer. The solenostomes of virgins were barely discernible, thus necessitating observation through the separation of mating pairs. Furthermore, it was observed that the spermatodactyl (broken) of the male was detached within the solenostomes (Figure 1).

The major duct was directly connected to the solenostomes and extended internally. The duct surface exhibited smoothness and some folding patterns. It maintained a regular shape characterized by thick, dense walls composed of multiple layers of cuticle. The cuticle appeared smooth, while the lumen within the duct was filled with a high-density material (Figure 2C).

The embolus connected the calyx and the major duct, starting from the major duct to the calyx. It was shorter in diameter and length than the major duct and calyx (Figure 2D).

Compared with both emboli and major ducts, an elongated calyx exhibits a folded surface structure (Figure 2E). The calyx exhibited a thick, uniform cuticle that typically assumed a circular shape but might display additional folds due to adjacent tissue pressure. At 10 and 12 h post-mating, the calyx exhibited content, with the presence of mitochondria observed in the calyx at 12 h post-mating (Figure 3B,D).

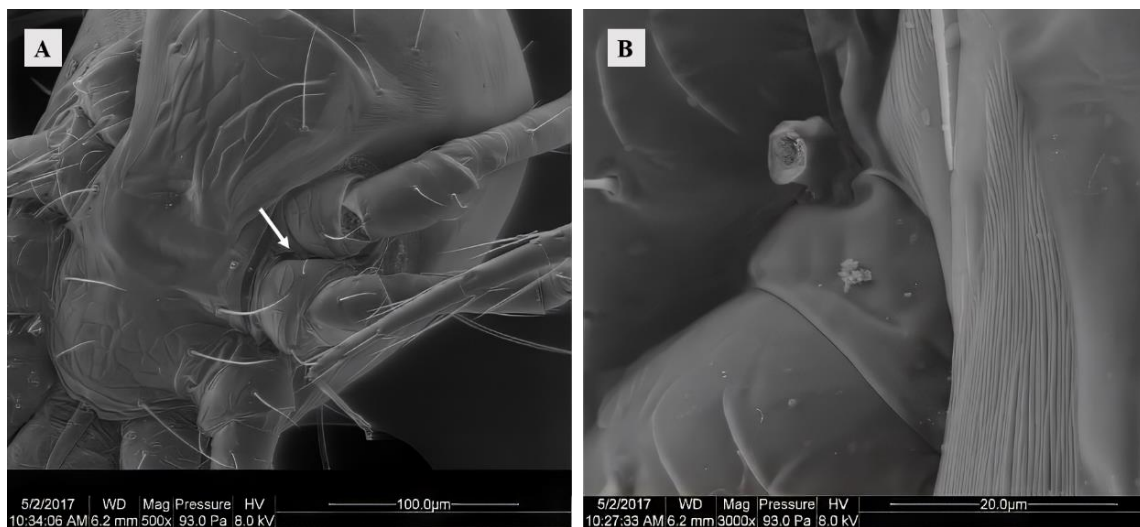


Figure 1. (A) SEM of the solenostomes of *Ph. persimilis* at 0 h after mating. Scale bar: 100 μ m. (B) A part of the chelicerae that was severed inside the Solenostome of *Ph. persimilis* during mating. Scale bar: 20 μ m. White arrow: solenostomes.

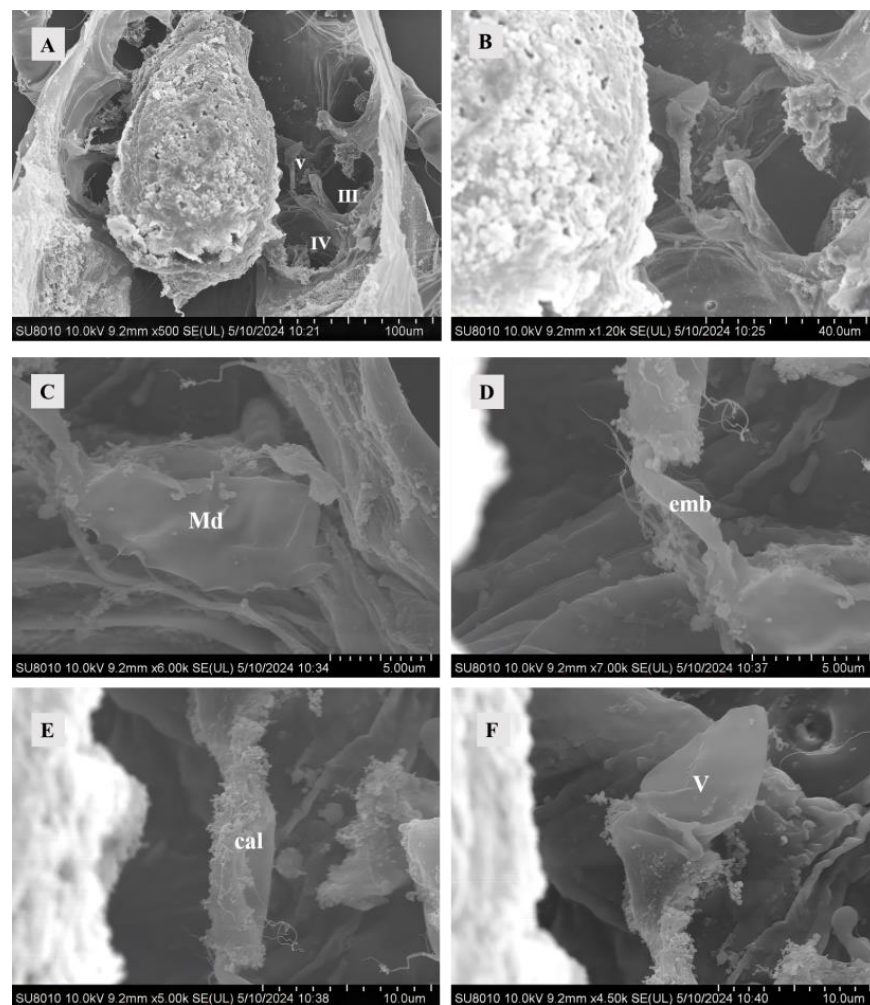


Figure 2. SEM of female sperm-access system at 0 h after mating. (A) The interior of *Ph. persimilis*. Scale bar: 100 μ m. (B) Sperm-access system. Scale bar: 40.0 μ m. (C) Major duct. Scale bar: 5.00 μ m. (D) Embolus. Scale bar: 5.00 μ m. (E) Calyx. Scale bar: 10.0 μ m. (F) Vesicle. Scale bar: 10.00 μ m. Abbr: cal, calyx; emb, embolus; Md, major duct; V, vesicle; III, IV: the third and the fourth leg.

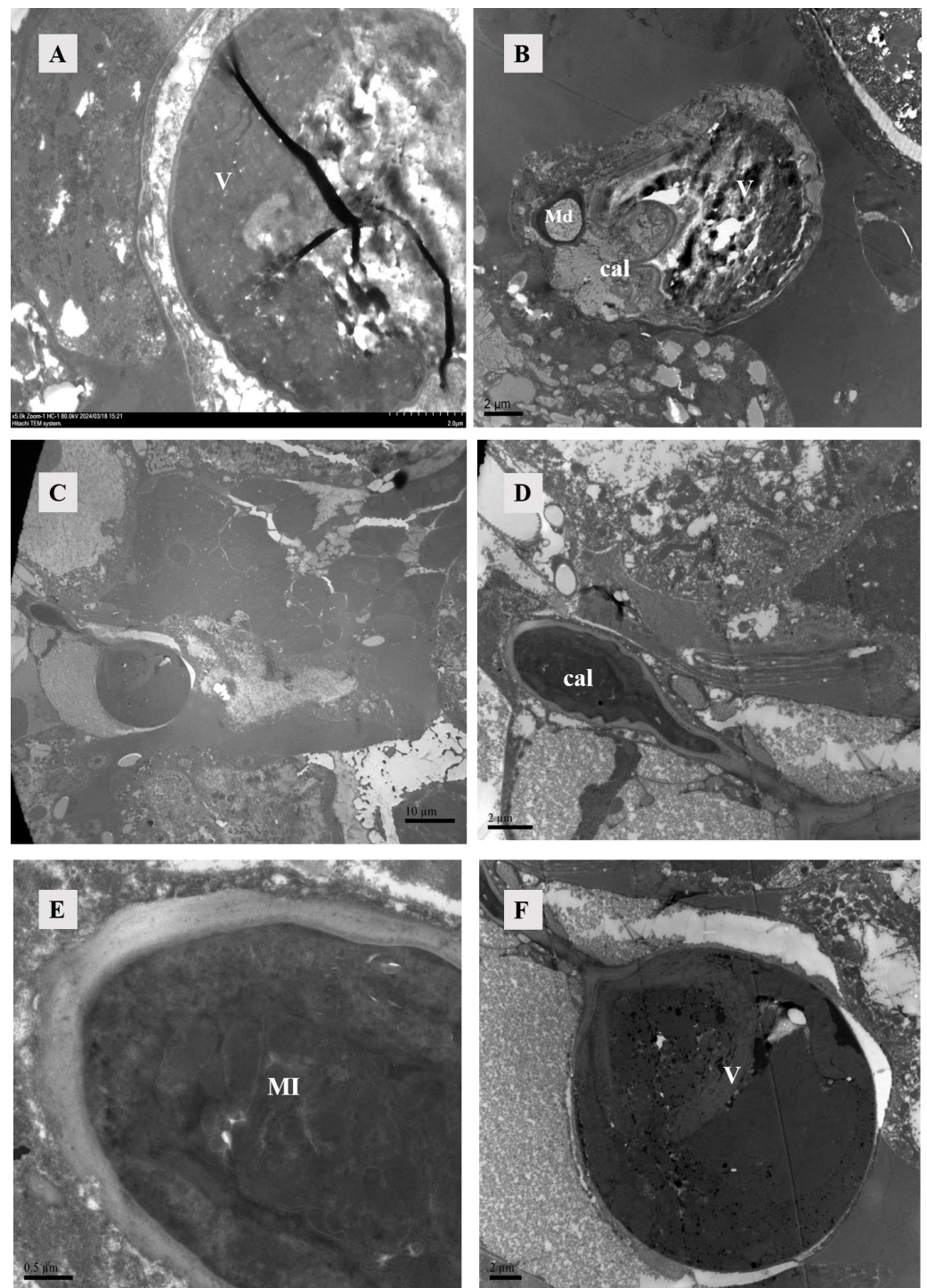


Figure 3. TEM of sperm-access system. (A) The vesicles at 4 h post-mating exhibited enhanced wall thickness and increased density within them. Scale bar: 2 μ m. (B) After 10 h of mating, the vesicle, major duct, calyx, and vesicle were simultaneously observable, with the vesicle also containing high-density material. Scale bar: 2 μ m. (C) Calyx and vesicle were observed in female individuals 12 h after mating. Scale bar: 10 μ m. (D,E) The calyx, observed 12 h after mating, exhibited a thick cuticle and a substantial presence of mitochondria. Scale bar: 2 μ m; 0.5 μ m. (F) The vesicles at 12 h after mating, in contrast to those observed at 4 h and 10 h after mating, exhibited the presence of a small vesicle characterized by a thick wall and were additionally filled with high-density material. Abbr: cal, calyx; Md: major duct; MI: mitochondria; V: vesicle.

The diagram depicted the vesicle of a recently mated female, as observed under an SEM, exhibiting a folded surface in an unfilled state. This structure remained imperceptible under TEM (Figure 2F). However, at 4, 10, and 12 h post-mating, the vesicle became filled with densely packed material (Figure 3). Females might manifest two states for their vesicles filled or unfilled. The wall of the smaller vesicle exhibited multiple layers of cutin, and the contents were densely packed (Figure 3F).

3.1.2. Lyrate Organ and Ovaries

After hematoxylin and eosin staining, the lyrate organ exhibited a predominant bluish-violet hue, while the ovaries displayed lighter bluish-violet. The centrally located lyrate organ was characterized by its large size and division into left and right parts, forming an incomplete saddle shape (Figure 4). The comparison of the lyrate organ within females at different mating times revealed that the lyrate organ at all mating stages contained nuclei. These nuclei were relatively large, with prominent nucleoli, irregular chromatin, and a large number of mitochondria. There was also evidence of nuclear fusion within lyrate organs (Figure 5). However, the nuclei showed differences between mated and unmated females. In virgins, the nuclei were underdeveloped, filled with heterochromatin, dispersed chromatin, and no nucleoli, and surrounded by numerous mitochondria (Figure 5A). In contrast, 4 h, 10 h, and 12 h after mating, the nuclei of the lyrate organs were well-developed, with prominent nucleoli, more condensed chromatin, no mitochondria inside the nuclei, and mitochondria uniformly distributed throughout the organs (Figure 5B–D).

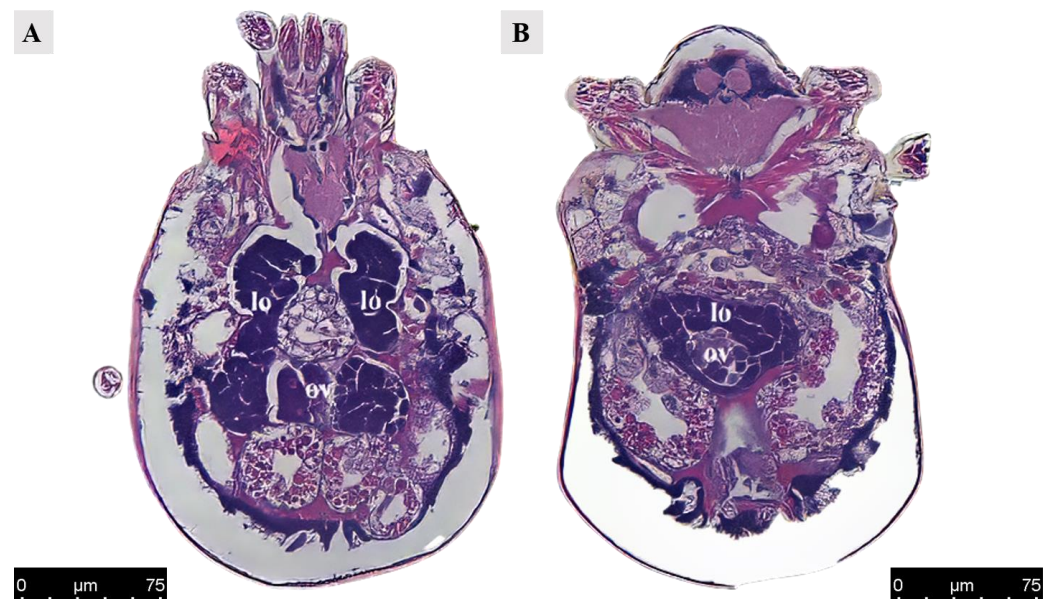


Figure 4. Paraffin section of ovary and lyrate organ in *Ph. persimilis* female at 12 h after mating. (A) The ovaries were positioned adjacent to the posterior region of the lyrate organ and are enveloped, as observed in a transverse view parallel to the abdomen. Scale bar: 75 µm. (B) Transverse section image perpendicular to the abdomen also revealed that the ovaries were surrounded by lyrate organ. Scale bar: 75 µm. Abbr: lo, lyrate organ; ov, ovary.

The ovary contained numerous somatic cells, and their morphology was mainly related to the stage of the surrounding oocytes, rather than the mating status. Compared to unmated females, we found that early-stage oocytes, 4 h, 10 h, and 12 h after mating, were surrounded by somatic cells with large nuclei but no prominent nucleoli. The cytoplasm was underdeveloped and contained abundant heterochromatin. Each oocyte was accompanied by two-to-three of these somatic cells. In later stages, the surrounding somatic cells increased in size and had dense cytoplasm with prominent nucleoli (Figure 6). At 10 h post-mating, an electron-transparent tissue was observed at the bottom of the ovary,

featuring a circular structure with rich granular material in mitochondria and endoplasmic reticulum (Figure 7).

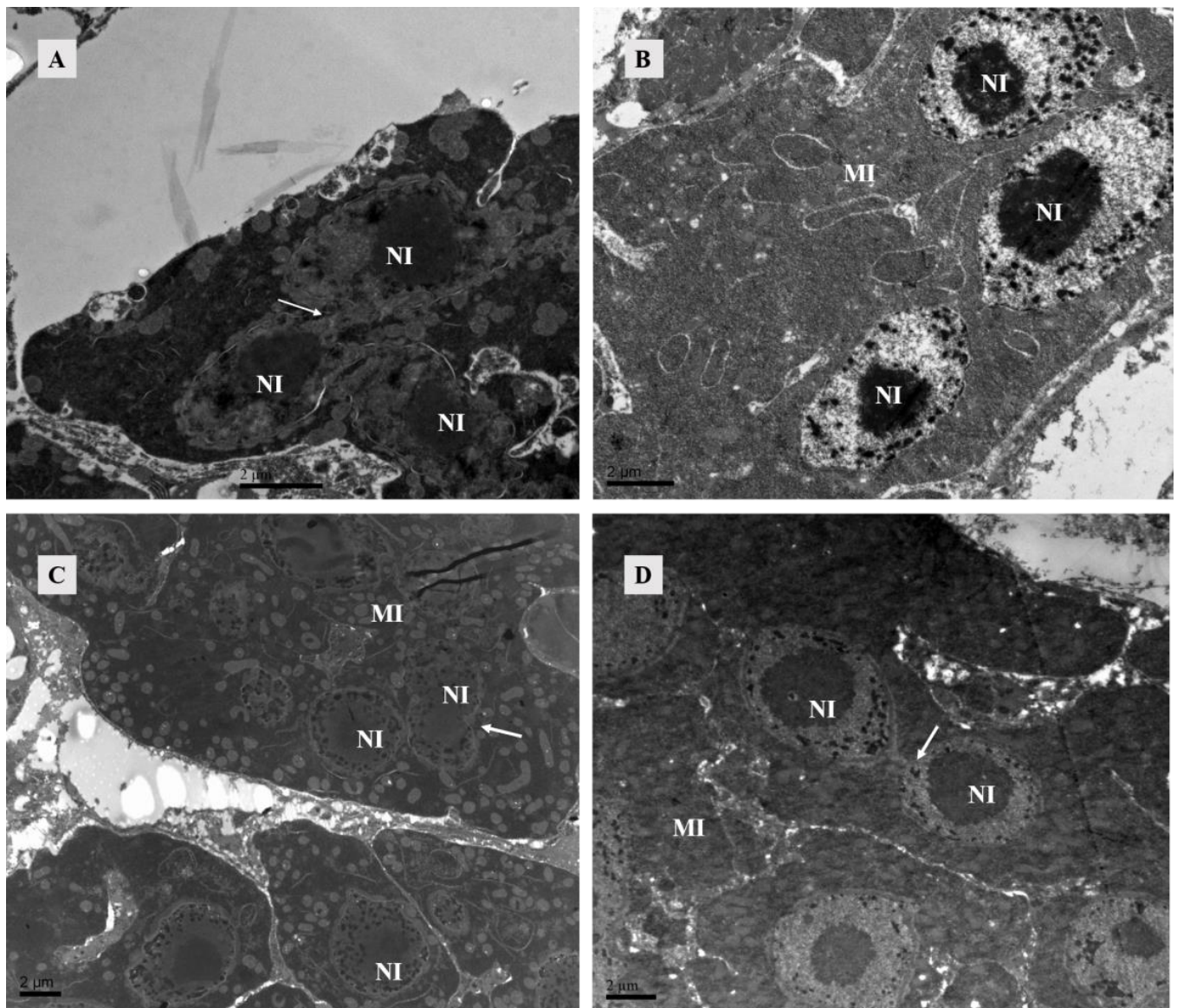


Figure 5. TEM of lyrate organ of *Ph. persimilis*. (A) The lyrate organ of unmated female mites exhibited an underdeveloped cell nucleus at this stage, characterized by the absence of a prominent nucleolus and dispersed heterochromatin within the nucleus. Additionally, mitochondria were predominantly localized in close proximity to the cell nucleus. Arrows show nuclei fusing with each other. Scale bar: 2 µm. (B–D) These were the lyrate organs of female mites at 4 h, 10 h, and 12 h post-mating. Throughout these three stages, the cell nuclei progressively undergo complete development with intact morphology and well-defined boundaries. The nucleoli exhibited distinct characteristics, accompanied by heterochromatin aggregation within the nucleus. Fusion phenomena between cells have been observed. A substantial number of mitochondria were uniformly distributed in the periphery of the lyrate organs; no intranuclear presence of mitochondria was detected. Scale bar: 2 µm. Abbr: MI, mitochondria; NI, nucleus of lyrate organ. Arrows show nuclei fusing with each other.

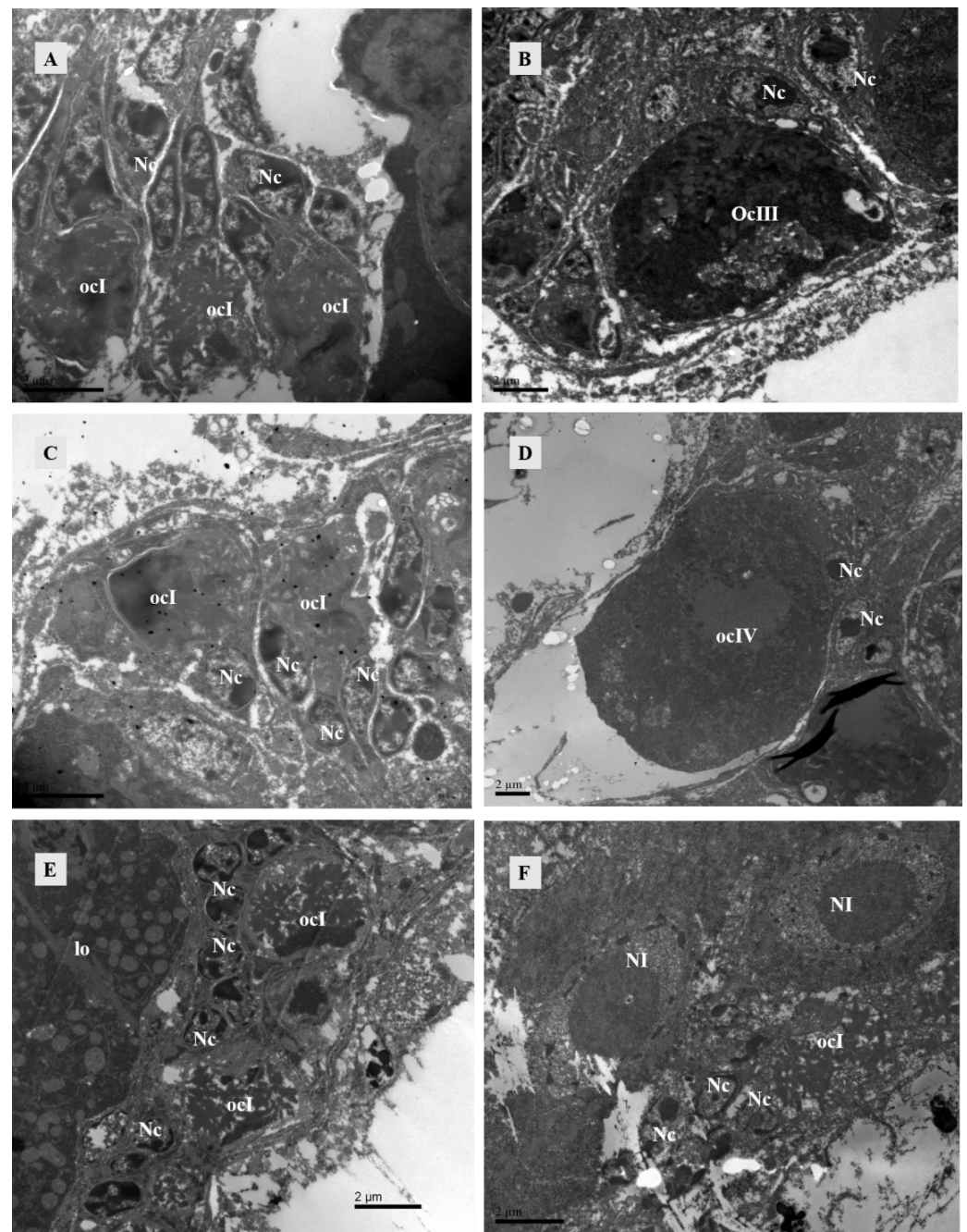


Figure 6. TEM of the ovary of *Ph. persimilis*. (A) Somatic cell nuclei surround the early oocytes in the ovaries of unmated female mites. These nuclei exhibited larger size, lack distinct nucleoli, possessed underdeveloped cytoplasm, and contained abundant heterochromatin. Each oocyte was accompanied by two-to-three such somatic cells. Scale bar: 2 μm . (B) The nuclei of somatic cells surrounding the mature oocytes in the ovaries of unmated female mites exhibited an increase in volume, accompanied by a densification of cytoplasm and distinct nucleoli formation. Scale bar: 2 μm . (C) After a 4 h mating period, the somatic cell nuclei surrounding the early oocytes in the ovaries of female mites also displayed incomplete development and exhibited diverse morphologies, characterized by an abundance of heterochromatin within their nuclei. Scale bar: 2 μm . (D) Peripheral somatic cells around the mature oocyte in the ovary of female 4 h after mating. The nuclei of somatic cells had clear boundaries and prominent nucleoli. Scale bar: 2 μm . (E,F) After 10 and 12 h of mating, the somatic cell nuclei surrounding the early oocytes in the ovaries of female mites were observed. These nuclei exhibited a similar structural composition to those found in the early oocytes during the preceding two developmental stages. However, due to ovary compression caused by egg presence

within the female mite's body during these two mating stages, late-stage oocyte development could not be observed. Scale bar: 2 μm . Abbr: lo, lyrate organ; ocl: oocyte of stage I; oclIII: oocyte of stage III; oclIV: oocyte of stage IV; Nc, nucleus of cup cell; NI, nucleus of lyrate cup.

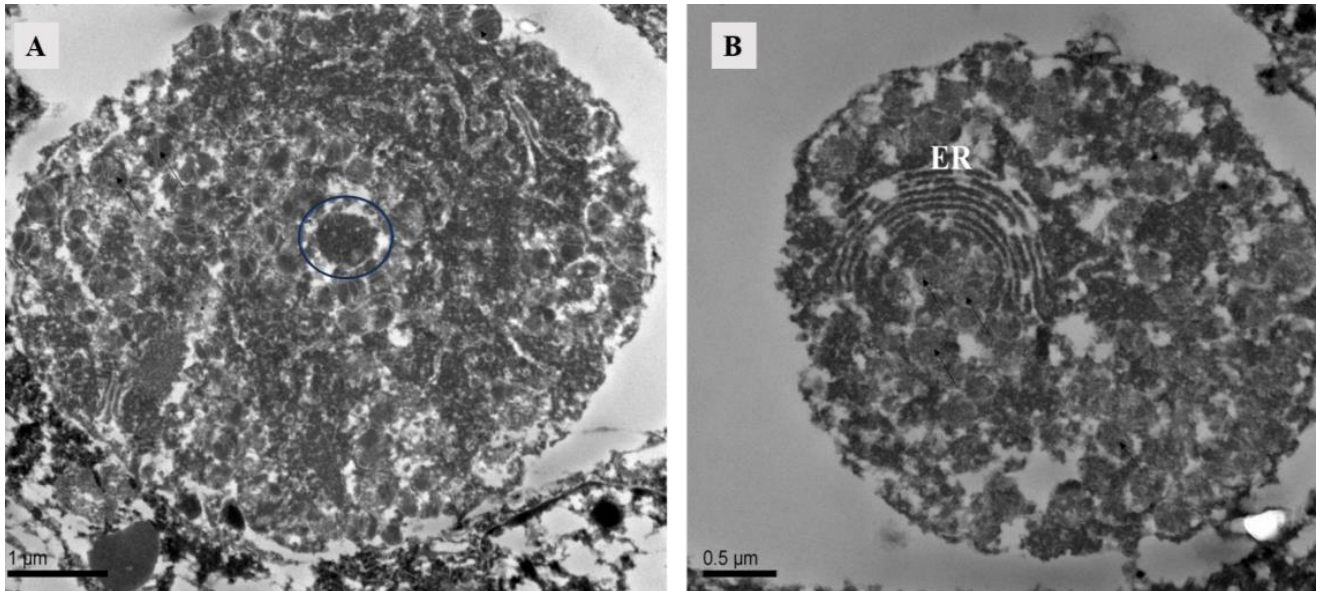


Figure 7. TEM of ovary at 10 h after mating of *Ph. persimilis*. (A) The electron-transparent tissue located below the ovaries contains circular structures. Scale bar: 1 μm . (B) Endoplasmic reticulum in electron transparent tissue. Scale bar: 0.5 μm . Abbr: ER, endoplasmic reticulum; blue circle, granular material.

3.1.3. Uterus, Vagina, and Genital Pore

When unfertilized, the uterus contracted (Figure 8A). After fertilization, it expanded to accommodate developing eggs (Figure 8B). Twelve hours after mating, eggs were present in the uterus (Figure 8C), and the uterine epithelium compressed into a thin layer and contained mainly endoplasmic reticulum and mitochondria (Figure 9A,B).

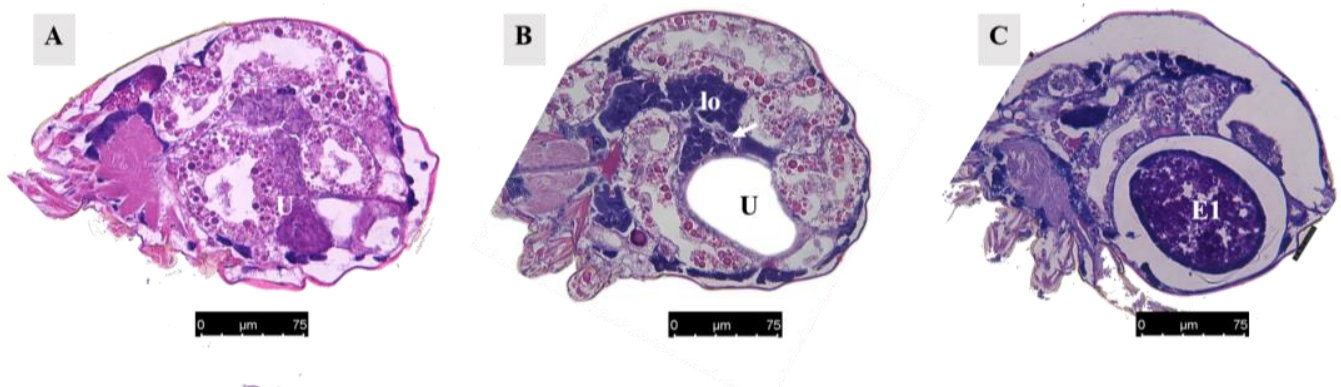


Figure 8. Paraffin section of the uterus. (A) Uterus of unmated female mite. Scale bar: 75 μm . (B) Uterus of female mite 13 h after mating. The white arrow represents the ovary. Scale bar: 75 μm . (C) Uterus of female mite 15 h after mating. Scale bar: 75 μm . Abbr: E1, the first egg; lo, lyrate organ; U, uterus.

The vagina is connected to the uterus. After the eggs matured in the uterus, the reproductive plate opened, allowing the eggs to be expelled through the vagina (Figure 9C).

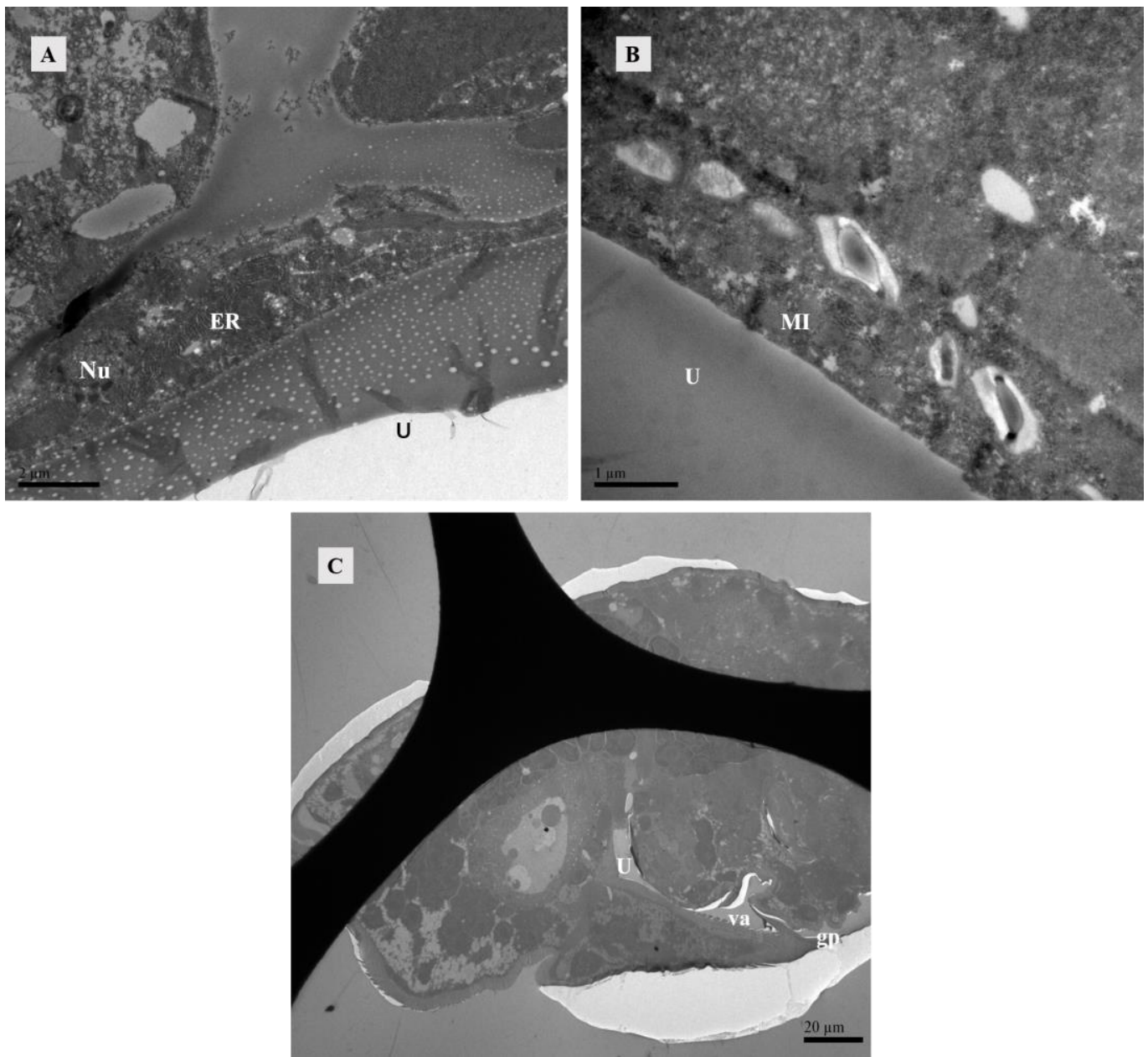


Figure 9. TEM of lyrate organ at 12 h after mating of *Ph. persimilis*. (A,B) The presence of eggs in the uterus resulted in compression of uterine epithelial cells, thereby exposing the structures of cell nucleus, endoplasmic reticulum, and mitochondria within these cells. Scale bar: 2 µm; 1 µm. (C) Longitudinal section image perpendicular to the abdomen. After 12 h of mating, when eggs were present in the body, the vagina and genital pore could be observed. Scale bar: 20 µm. Abbr: ER, endoplasmic reticulum; gp, Genital opening; MI, mitochondria; Nu, Uterine epithelial cell nucleus; U, uterus; va, vagina.

3.2. Spatial Relationships between Structures

The posterior part of the lyrate organ was enclosed and connected to the ovary, forming a surrounding structure. The anterior part of the lyrate organ was adjacent to and closely connected with the vesicle, which was enveloped and embedded within it (Figures 4 and 10A,B). Positioned beneath the ovary, the uterus expanded when filled with eggs, occupied almost all of the abdominal cavity, and exerted pressure on the periphery of the lyrate organ (Figures 8B and 10C).

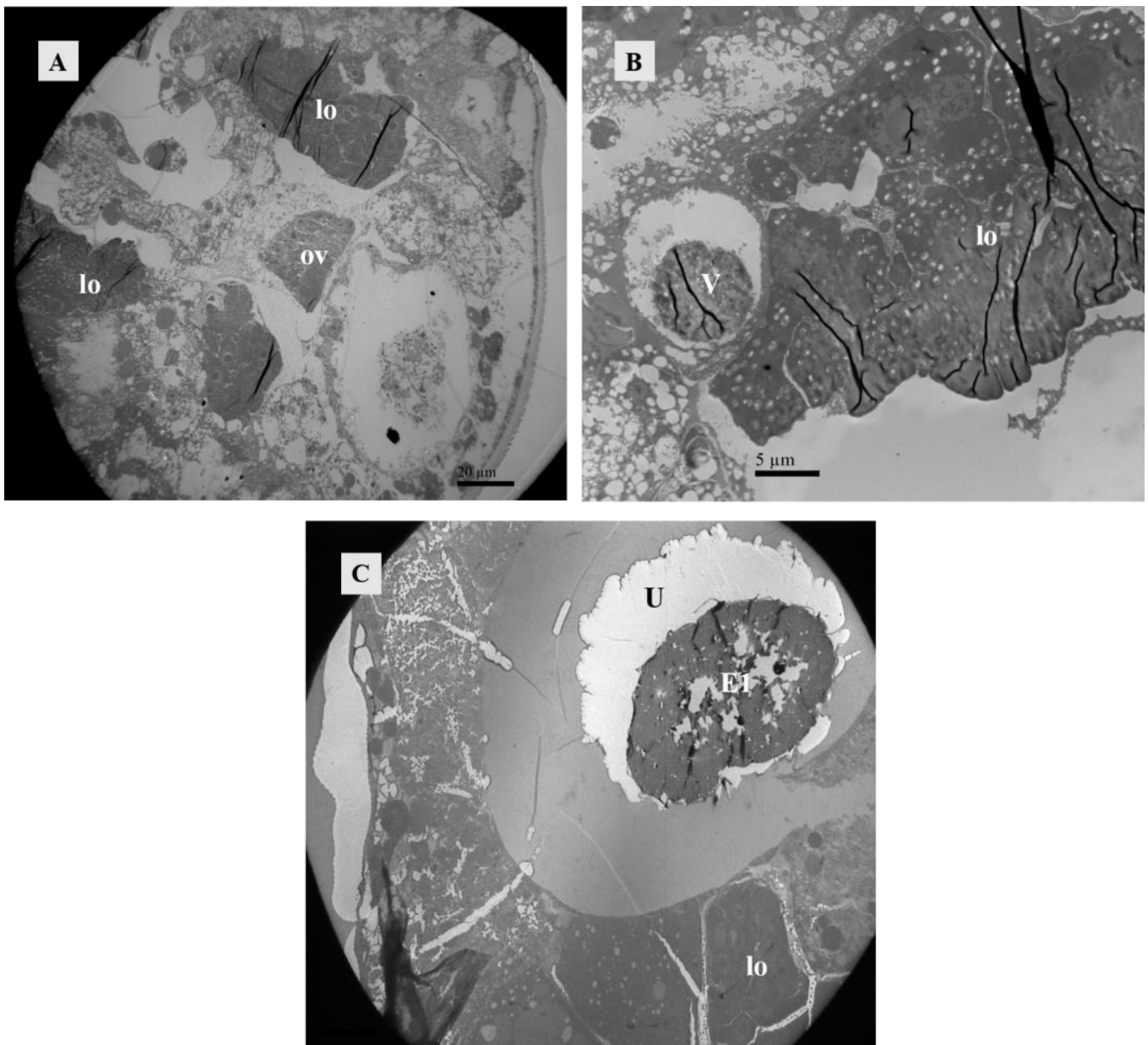


Figure 10. Position relationship between ovary, vesicle, and lyrate organ. (A) Female mite 4 h after mating. Transverse section image parallel to the abdomen. The posterior half of the ovary was adjacent to the uterine organ and surrounded by it. Scale bar: 20 μm . (B) Female mite 4 h after mating. Transverse section image perpendicular to the abdomen. The vesicle was situated within the lyrate organ, and it was enclosed by the anterior portion of the lyrate organ. Scale bar: 5 μm . (C) Female mite 12 h after mating, the presence of the first egg in the uterus was evident, exerting pressure on the uterine organ towards the body's periphery. Scale bar: 20 μm . Abbr: E1, the first egg; lo, lyrate organ; ov, ovary; U, uterus; V, vesicle.

3.3. The Development of Oocytes at Different Mating Times

In the ovaries of unmated female mites, four oocyte developmental stages were visible, including stage I, stage II, stage III, and stage IV. Within the ovaries, multiple oocytes in stage I were present. These cells exhibited significantly large nuclei that occupied almost the entire oocyte volume. A notable characteristic feature of these stage I oocytes was the presence of Star heterochromatin within their nuclei. Furthermore, cup cells surrounded the stage I oocytes (Figure 11A,B).

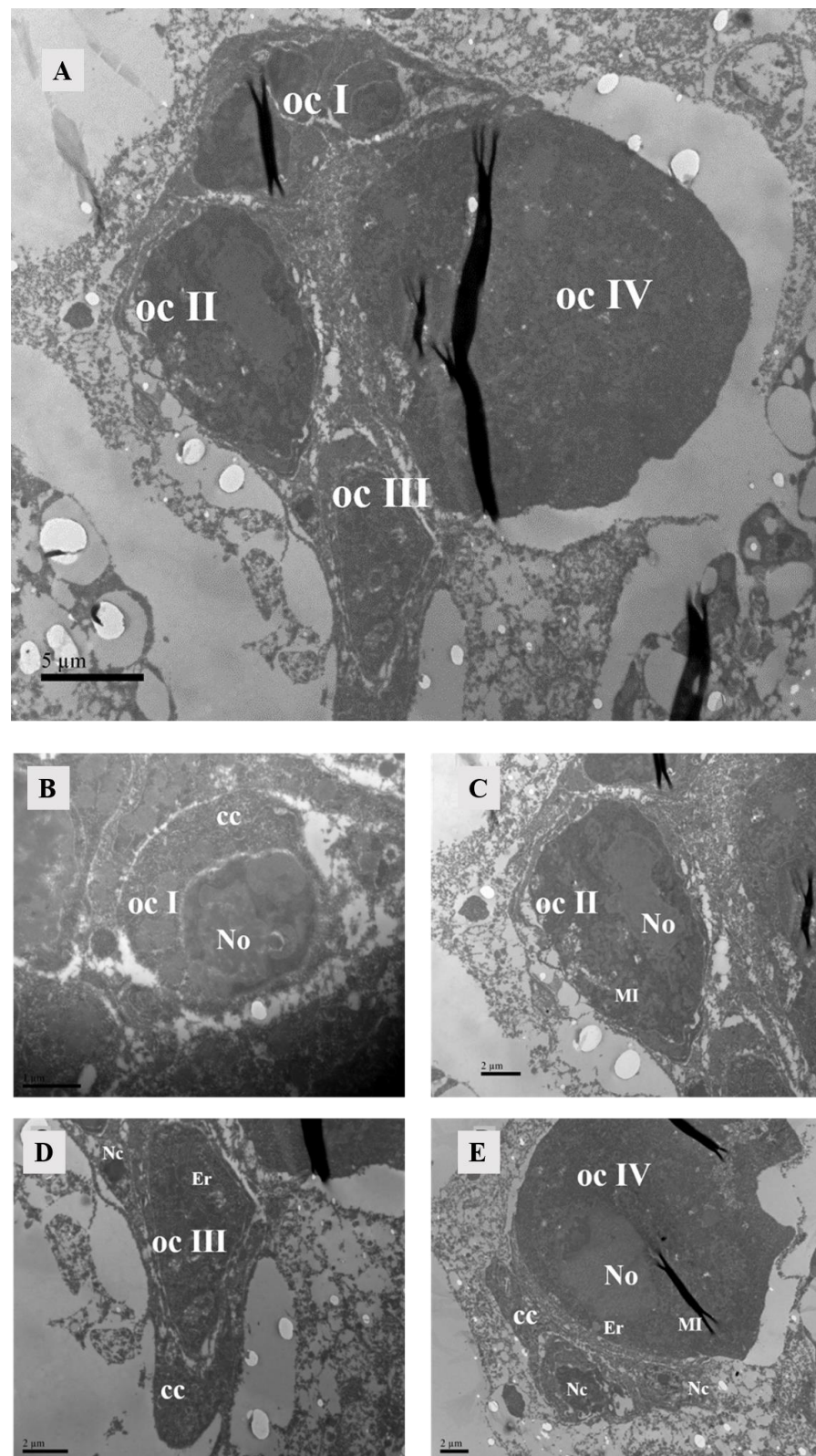


Figure 11. Oocyte in ovary of unmated female. (A) It could be seen that the oocytes were in four developmental stages. Scale bar: 5 µm. (B) Oocyte of stage I: The cell nucleus was relatively large, containing star-shaped heterochromatin within and cup cells surrounding the oocyte. Scale bar: 1 µm. (C) Oocyte of stage II: The nucleolus was homogeneous, and there were mitochondria inside the cell. (D) Oocyte of stage III, encompassing a substantial quantity of endoplasmic reticulum and mitochondria. (E) Oocyte of stage IV: The cell was abundant in mitochondria, endoplasmic reticulum,

and free ribosomes. Scale bar: 2 μm . Abbr: Er, endoplasmic reticulum; ocI, oocyte of stage I; ocII, oocyte of stage II; ocIII, oocyte of stage III; ocIV, oocyte of stage IV; No, nucleus of oocyte; Nc, nucleus of cup cell; cc, cup cell, MI, mitochondria.

Oocytes at developmental stage II were larger in size and possess a homogeneous nucleolus. The nuclear volume decreased compared to that of stage I oocytes during this phase. Numerous organelles included free ribosomes, and irregularly shaped mitochondria appeared within the ooplasm (Figure 11C).

At developmental stage III, the oocyte volume further increased. In comparison to stage II, there was a greater diversity and abundance of organelles, including substantial amounts of endoplasmic reticulum and mitochondria. At this stage, the oocyte was enveloped by two cup cells: one located at one pole of the oocyte and the other encircled the oocyte with a prominent nucleolus (Figure 11D).

During developmental stage IV, the oocyte attained its maximum size, exhibiting abundant cytoplasm and harboring the highest number of organelles among all four stages. It was replete with numerous mitochondria, endoplasmic reticulum structures, and free ribosomes (Figure 11E). The presence of oocytes at all four developmental stages in unmated female mites indicated that even in an unmated state, oocyte development initiates. With exception to stage I, where multiple oocytes were observed simultaneously, our study revealed only one single oocyte present during each subsequent stag.

Observations of *Ph. persimilis* 4 h after copulation revealed that oocytes at four different developmental stages were still present in the ovaries, with morphology similar to that of unmated mites. The presence of oocytes at various developmental stages remained consistent in the ovaries regardless of mating status, with no notable disparities observed between mated and unmated mites (Figure 12). After copulation, the ovaries exhibited oocytes at various stages of development. By 7 h post-copulation, the ovaries contained two oocytes and two developing eggs. At 10 h post-copulation, two oocytes and two developing eggs could be observed. At 12 h post-copulation, the ovaries contained three oocytes and two developing eggs (Figure 13).

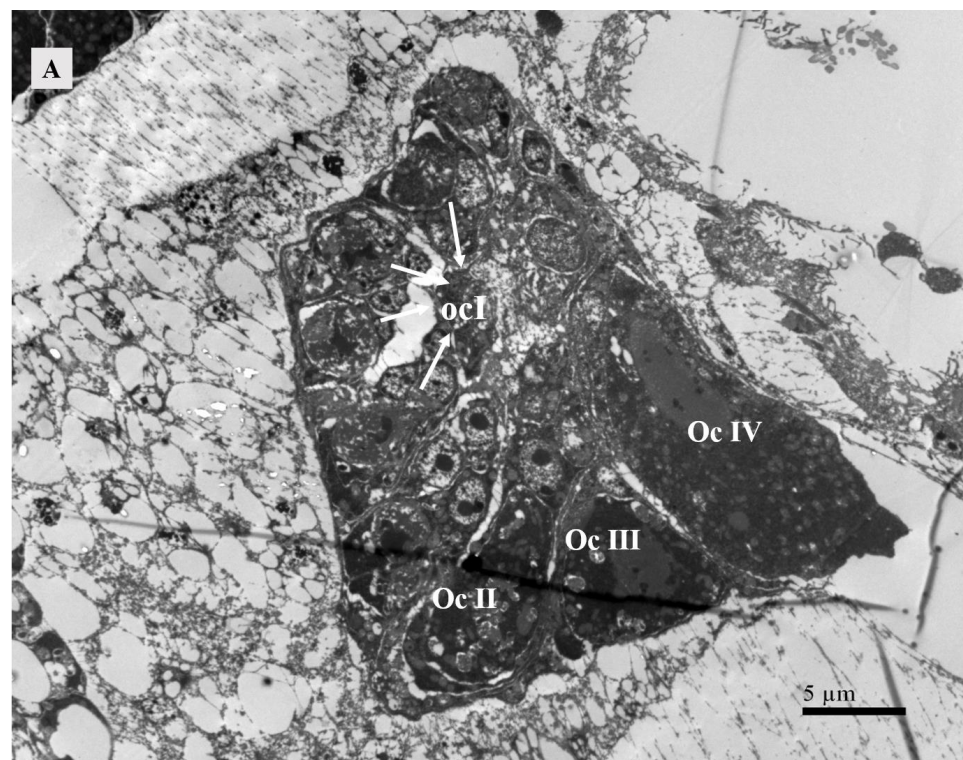


Figure 12. Cont.

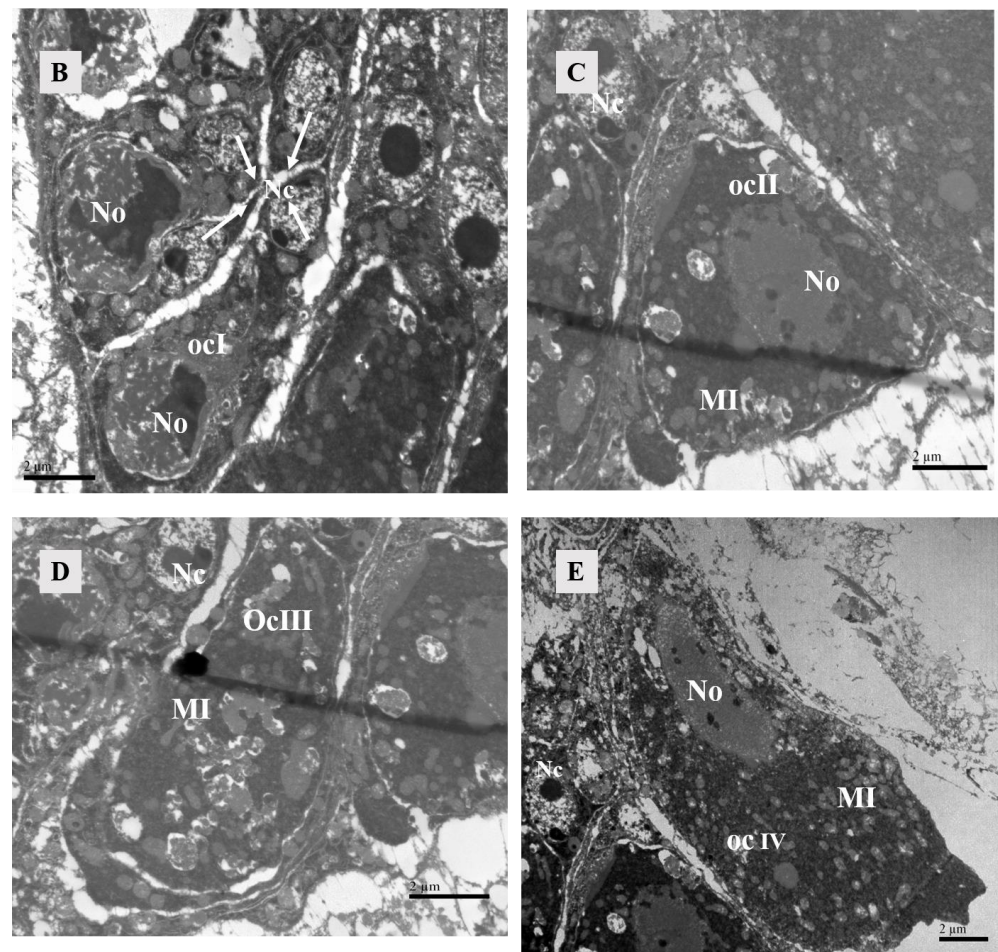


Figure 12. Oocytes in the ovary of female at 4 h after mating. (A) Four stages of oocyte development could be observed within the ovary. Scale bar: 5 µm. The white arrow represented oocyte of stage I. (B) Oocyte of stage I: Each oocyte was surrounded by two to three cup cells. Scale bar: 2 µm. The white arrow represented nucleus of cup cell. (C) Oocyte of stage II: The nucleus of the oocyte forms, and there were mitochondria inside the cell. Scale bar: 2 µm. (D) Oocyte of stage III: No intact oocyte nuclei were observed, possibly due to the slicing process. Scale bar: 2 µm. (E) Oocyte of stage IV: The nucleus of the oocyte was elongated in shape, with heterochromatin present within the nucleus. Scale bar: 2 µm. Abbr: MI: mitochondria; No, nucleus of oocyte; Nc, nucleus of cup cell. ocI, oocyte of stage I; ocII, oocyte of stage II; ocIII, oocyte of stage III; ocIV, oocyte of stage IV.

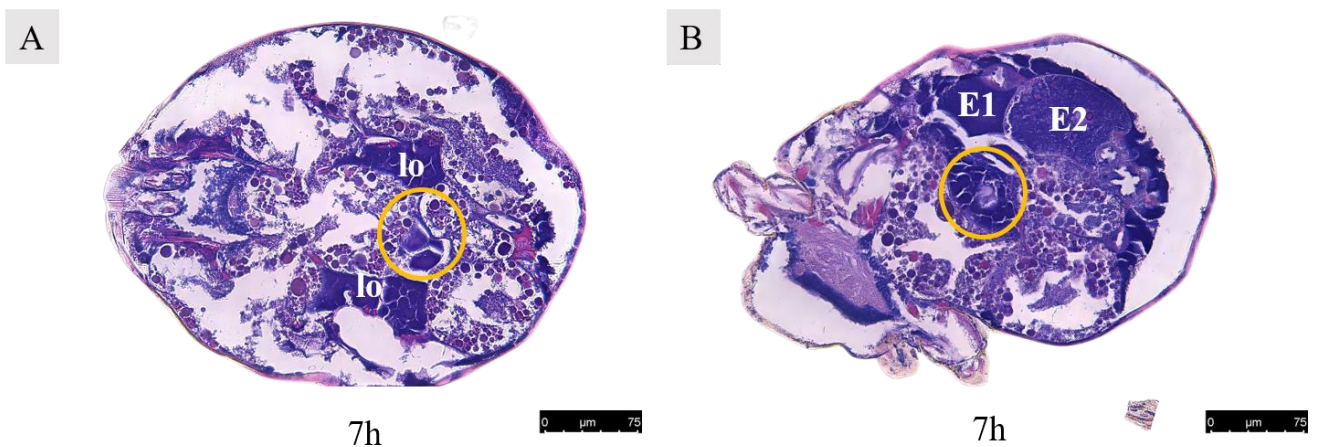


Figure 13. Cont.

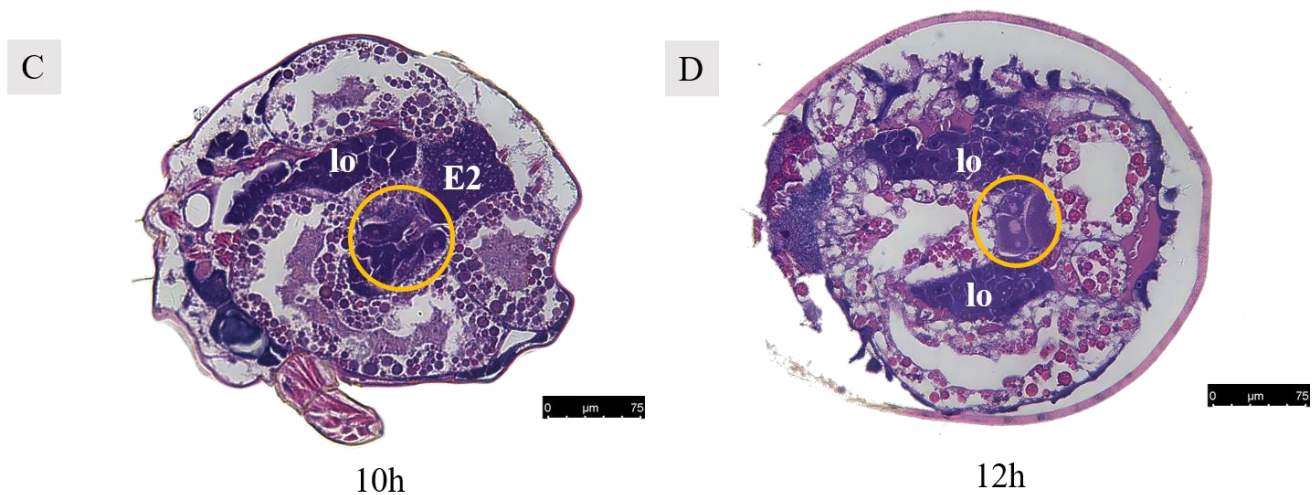


Figure 13. Paraffin sections of *Ph. persimilis* female at different mating periods. (A,B) After 7 h of mating, two egg cells and two developing eggs were observed in the ovaries. (C) After 10 h of mating, two oocytes and the second polar body in the ovaries. (D) After 12 h of mating, three oocytes and two developing eggs in the ovaries. Abbr: E1, the first egg; E2, the second egg; lo, lyrate organ; yellow circle, oocyte in the ovary. Scale bar: 75 μm .

3.4. Egg Formation

3.4.1. Development of the First Egg (Figure 14)

Observations were conducted on *Ph. persimilis* at 18 different time points, ranging from the unmated state to the first egg laying, using paraffin-sectioning techniques. In unmated female mites, the uterus was not visible.

At 1 h post-mating, a distinct space became apparent in the ovaries. However, no egg formation was observed. By 2 h post-mating, oocytes begin entering the yolk development phase, characterized by yolk granules aggregating around a contracted nucleus. At 4 h post-mating, eggs exhibited enlarged and densely packed yolks without any gaps as they started growing outward from the ovary towards the dorsal side.

By 6 h post-mating, the yolk continued to enlarge, and the egg remained positioned towards the dorsal side. From 7–9 h after mating, a critical period for yolk development in the first egg ensues. During this time frame, yolk synthesis occurred while the egg underwent rapid growth on its dorsal side. Although surrounded by a membrane, an irregular shape was observed due to the absence of a fully formed eggshell.

At 10 h post-mating, the first egg transitions from its initial dorsal position to reside within the uterus in the abdominal area. The presence of numerous yolk and lipid droplets could be noted. However, the complete formation of an eggshell had not yet occurred. Notably, four cells were discernible at the center of the egg, as indicated by black arrows in accompanying images. Subsequent to entering into the uterus, ongoing developmental processes continue within these eggs. Around 12–13 h of post-mating marked the initiation of eggshell formation, which imparts the final shape upon each individual egg. Following the completion of eggshell formation, extensive cell division commenced within each embryo, signifying the onset of embryonic development.

At 13–14 h post-mating, the egg exhibited cellular concentration at one pole, accompanied by abundant yolk and lipid droplets. By 15–16 h post-mating, cellular migration commenced from their initial position towards the eggshell periphery, forming a contiguous layer in close proximity to it. At 16 h post-mating, the first egg attained maturity with substantial internal contents. The cells aligned along the eggshell circumference, resulting in a discernible blue cell band. At this stage, the internal development of the first egg concludes, and it becomes primed for oviposition. Subsequently, upon the laying of the first egg, the second egg proceeded into the uterus for further maturation.

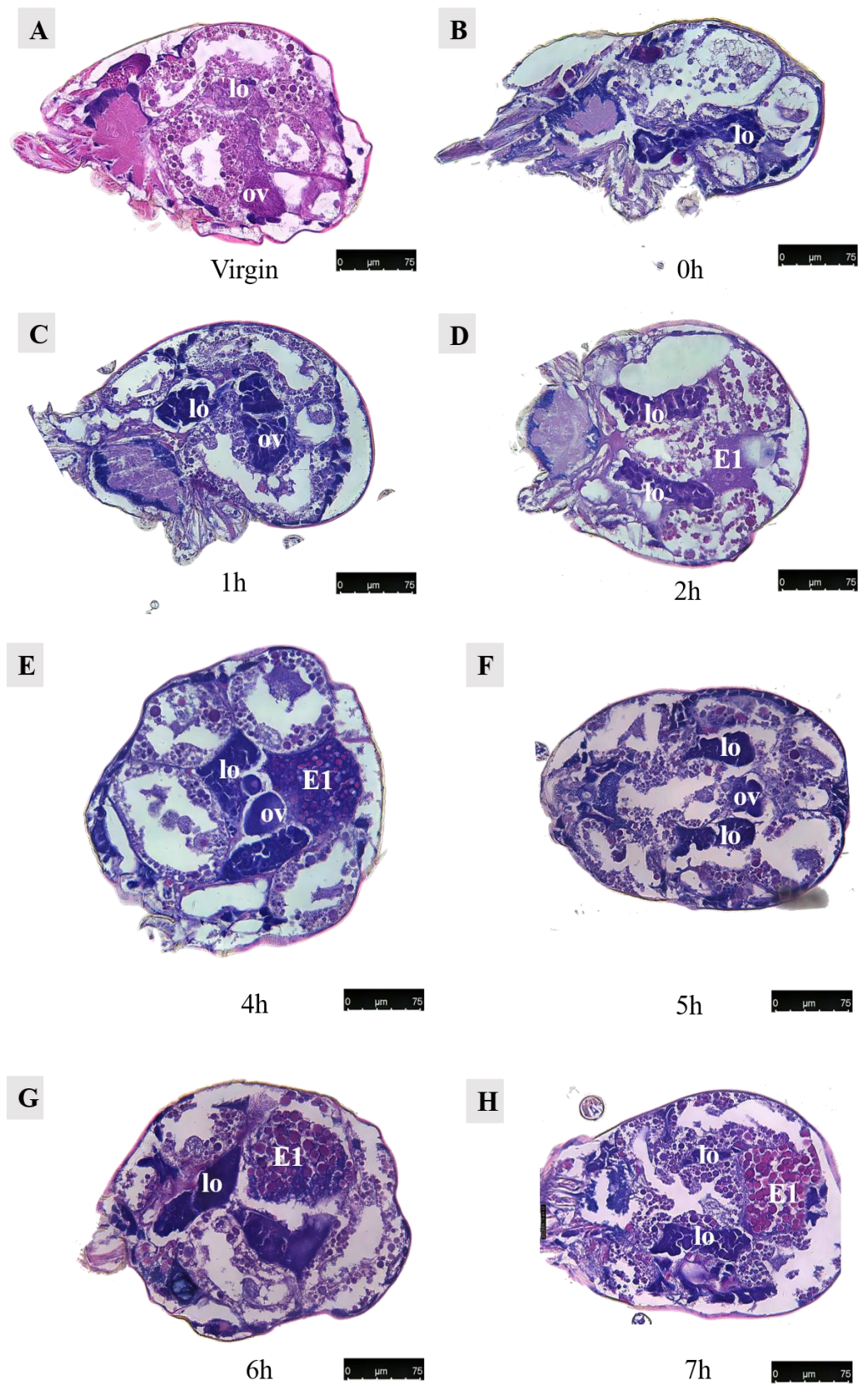


Figure 14. Cont.

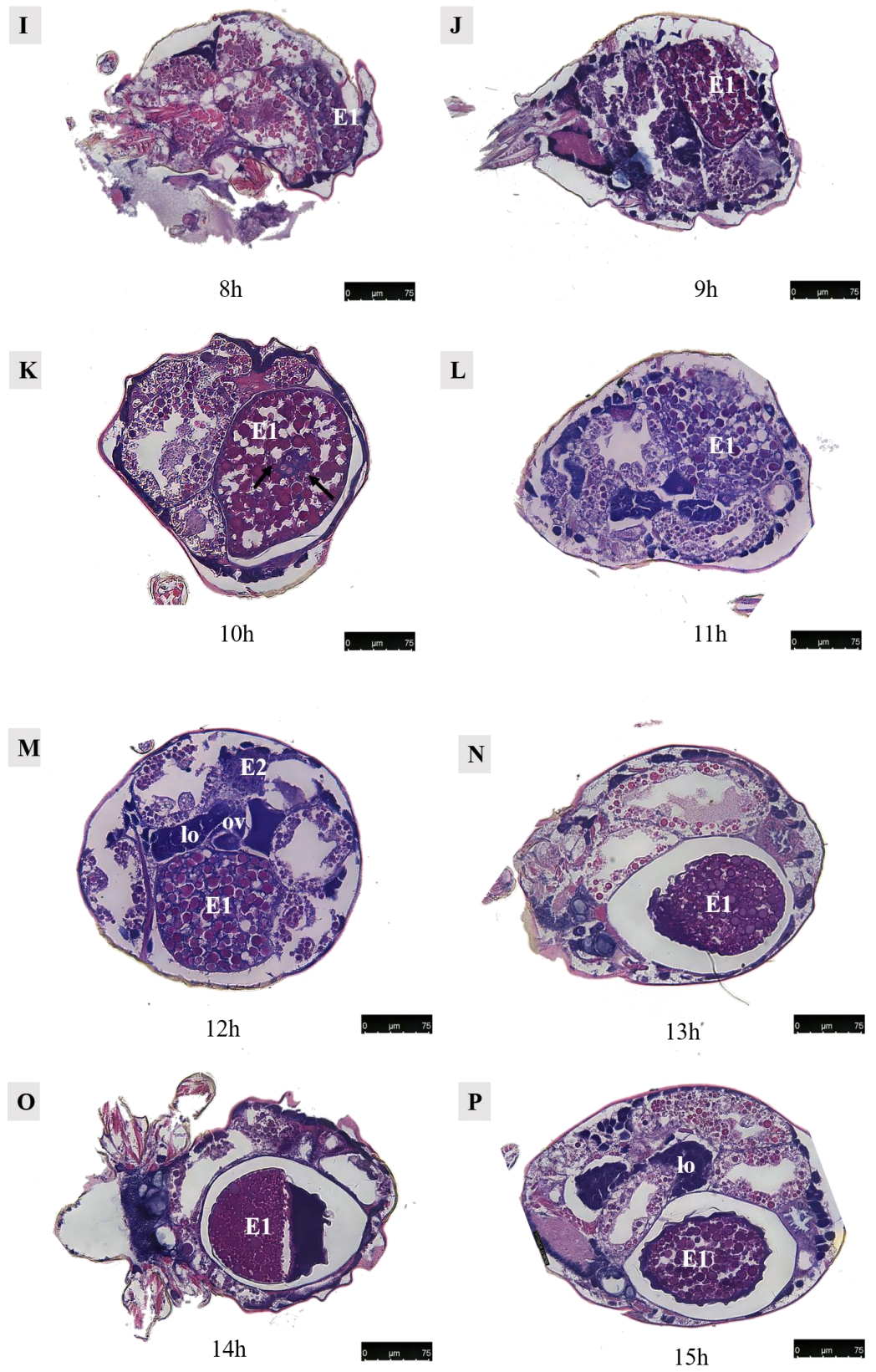


Figure 14. Cont.

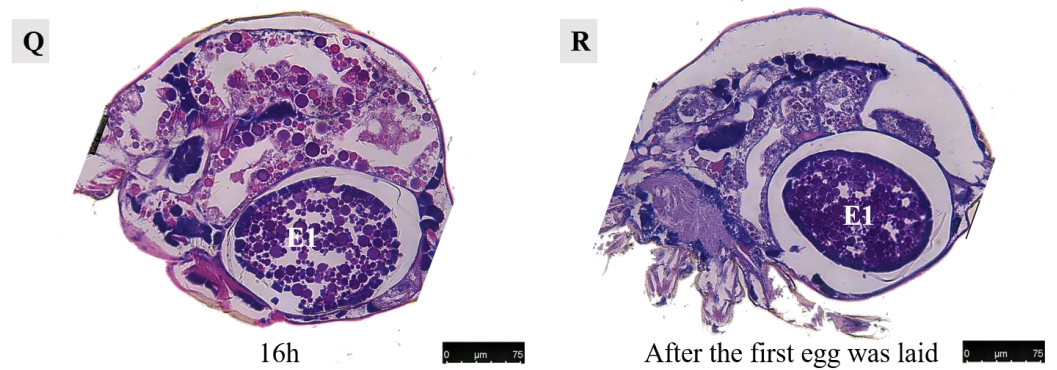


Figure 14. Paraffin sections of *Ph. persimilis* female at different time after mating. (A) Unmated female mite. (B) 0 h after mating. (C) 1 h after mating. (D) 2 h after mating. (E) 4 h after mating. (F) 5 h after mating. (G) 6 h after mating. (H) 7 h after mating. (I) 8 h after mating. (J) 9 h after mating. (K) 10 h after mating. (L) 11 h after mating. (M) 12 h after mating. (N) 13 h after mating. (O) 14 h after mating. (P) 15 h after mating. (Q) 16 h after mating. (R) 17 h after mating. Scale bar: 75 μ m. Abb: lo, lyrate organ; ov, ovary. E1, the first egg; E2, the second egg; black arrow: cells in the first egg.

3.4.2. Development of the Second Egg

After 7 h of mating, the second egg initiated development (Figure 13B). Following an additional 12 h period, three developing eggs became visible: the first egg was located within the uterus, the second egg was positioned near the dorsal side, and the third egg was situated above the uterus but still in the early stages of development (Figure 15A). Upon examination of a female 15 h after mating, it was observed that the first egg resided in close proximity to the abdominal side within the uterus, while the second egg was found outside of it near the dorsal side. Notably, spatial misalignment between these two eggs was evident. Furthermore, when dissecting a section perpendicular to the abdominal plate, only one discernible egg could be observed within the uterus (Figure 16).

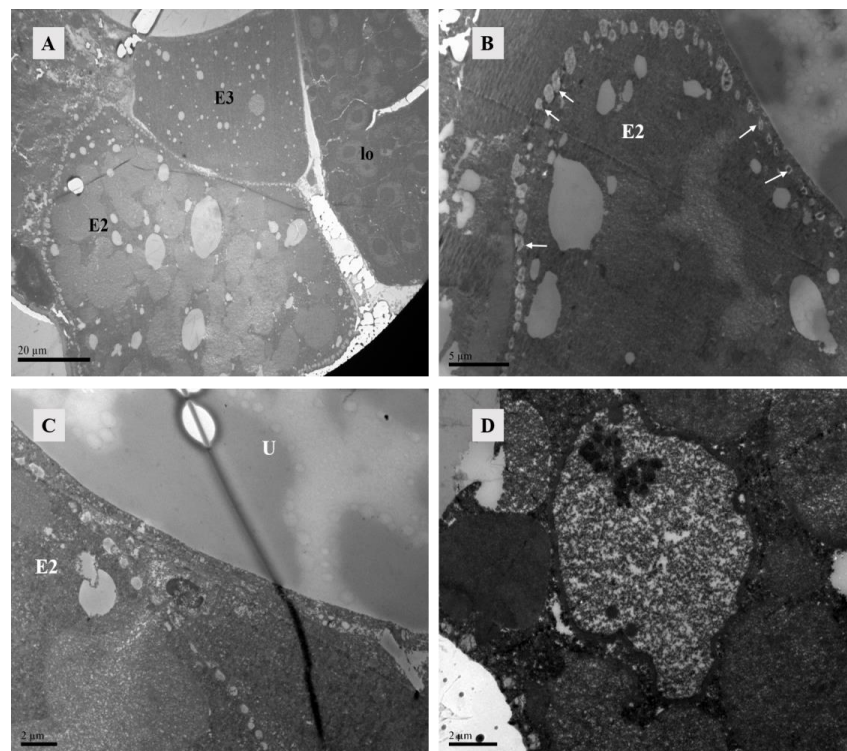


Figure 15. TEM of *Ph. persimilis* female at 12 h after mating. (A) Three developing eggs could be observed inside the posterior 12 female mites, and the lyrate organ was squeezed to the edge of the

body. Scale bar: 20 μm . (B) The second egg was surrounded by lipid vesicles. The arrow pointed to the lipid vesicles. Scale bar: 5 μm . (C) Near the uterus, there was a lipid vesicle on the edge of the second ovum. Scale bar: 2 μm . (D) The second egg had obvious membrane structures, containing a large number of free ribosomes within the structure. Scale bar: 2 μm . Abbr: E2, the second egg; E3, the third egg; lo, lyrate organ; U, uterus; white arrow: lipid vesicles.

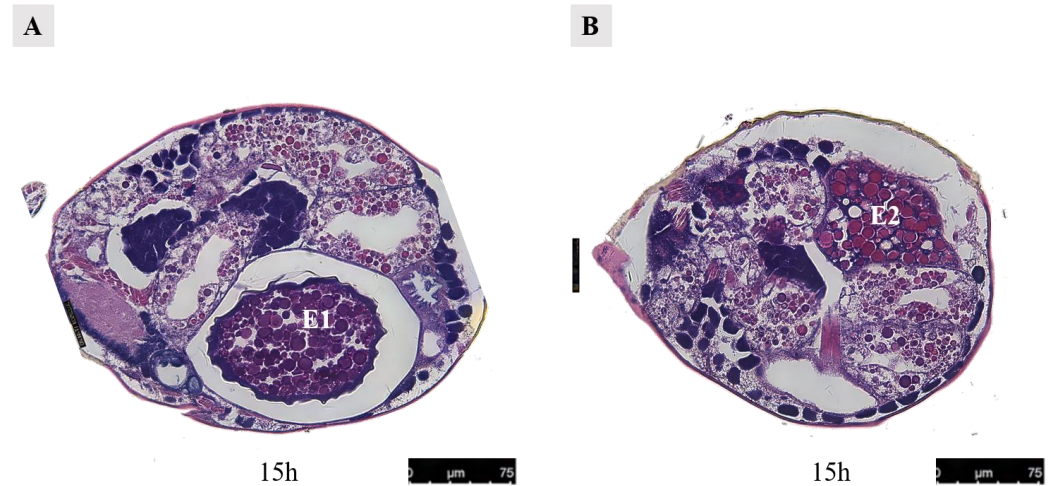


Figure 16. Paraffin section of the female at 15 h after mating in *Ph. persimilis*. (A) The first egg was inside the uterus, while the second egg outside the uterus was not visible. (B) The second egg was outside the uterus, while the first egg located inside the uterus was not visible. Scale bar: 75 μm . Abbr: E1, the first egg; E2, the second egg.

Lipid vesicles encircled the second egg completely. Lipid vesicles completely surround this second egg, which might represent an initial phase of eggshell formation since no other membrane structures were apparent. The second egg contained yolk primordial granules, lipids, and particulate matter (Figure 15B,C). Although distinct cells could not be observed yet, membrane structures contained darker and transparent materials, suggesting an incipient cellular formation (Figure 15D).

3.5. Embryonic Development

In *Ph. persimilis*, at 9 h post-mating, two cells could be seen in the first egg, analogous to the union of sperm and egg cells. Then, 10 h post-mating, the first egg in the uterus showed four cells at its center, suggesting early cleavage divisions. Sperm and egg fusion should occur between 9 and 10 h. By 13 h, the second egg contained a single cell. These could potentially be fused sperm cells derived from the second egg (Figure 17).

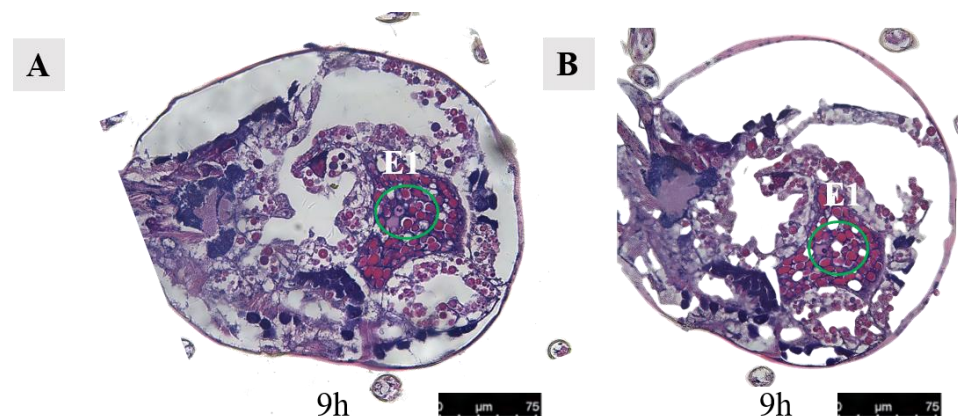


Figure 17. Cont.

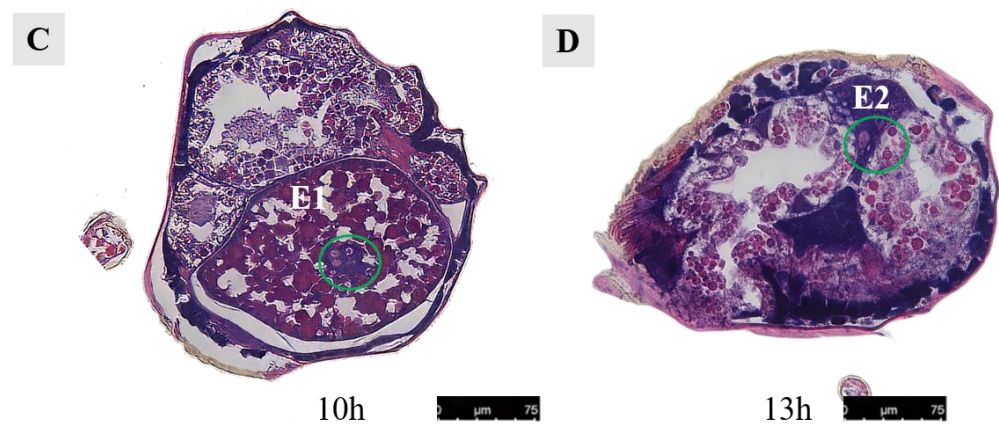


Figure 17. Cells in the abdominal eggs of the female mites in *Ph. persimilis*. (A,B) Female 9 h after mating. Inside the egg, two cells could be seen. (C) Female mite 10 h after mating. The first egg was transferred to the uterus, and four cells could be seen inside the egg. (D) Female mite 13 h after mating. There was a cell visible inside the egg. Scale bar: 75 µm. Abbr: E1, the first egg; E2, the second egg; the green circle, the cells in the egg.

4. Discussion

This study identified the reproductive structures in *Ph. persimilis* females, including paired solenostomes, major ducts, embolus, calyces, and vesicles within the sperm-access system. The unpaired gonads, the lyrate organ, and the ovary were also present. Consistent with previous research, it encompassed the uterus, vagina, and genital pore, which were involved in egg development and expulsion [5,18,19]. Although minor ducts in the sperm access were expected [7], they were not observed possibly due to their delicate structure being damaged or overlooked. Di Palma indicated that solenostomes located deeply within the basal segments of the third and fourth legs were challenging to observe. However, by scanning and separating the mating male mites, we observed the solenostomes in the female. The vesicle in female mites could be in either non-full or full states, which were related to the mating status and the level of sperm content [7]. Additionally, as the mating duration increases, the volume of the vesicle also increases [12]. In *Paurocephala sauteri* Enderlein, the vesicle's length and width increased by 1.74 and 1.84 times, respectively, before mating [20]. Similarly, in *Diaphorina citri*, the vesicle enlarged sequentially before, during, and after mating [21]. The vesicle showed densely packed contents, but it was unclear whether sperm cells were present. Previous studies have indicated the presence of a structure referred to as the "sperm package" or "internal sperm package" within the sperm reception system [22]. In Phytoseiidae, these internal sperm packages were observed in the vesicle during or shortly after mating [7]. Schulten [23] suggested that the internal sperm package gradually diminished within 1–2 days post-mating, while Doss [24] observed its high sclerotization and resistance to destruction even after exposure to lactic acid immersion and heating. Therefore, we hypothesized that the dense material present in the vesicle might correspond to the internal sperm package. In insects like *Diaphorina citri*, the vesicle expands and contains white sperm packages later in mating [21].

The morphology of the lyrate organs differed from Alberti and Hänel's description of Dermanyssina's [19] that mating had a significant impact on the morphology of the nuclei, but the duration of time after mating did not affect the nuclear morphology. But nuclear fusion indicated high ribosome or ribosomal precursor activity [7]. While detailed descriptions were lacking, the organ was believed to aid in nutrient supply [5,25]. Positioned anterior to the vesicle and posterior to the ovaries, the lyrate organ might also play a role in sperm transfer and ovary protection.

The morphology of somatic cells was primarily determined by the stage and distribution of surrounding oocytes within the ovary, rather than their mating status. This suggested that somatic cells predominantly served to support and protect the oocytes. Our

research demonstrated no discernible differences in the oocyte state across various mating conditions, indicating that different mating conditions did not exert an influence on somatic cell morphology. From a medical perspective, cup cells were involved in synthesizing and secreting mucins to establish a protective mucosal barrier for epithelial cells [26]. Similarly, in mites, cup cells potentially contributed to nourishing the developing oocytes and facilitating their transportation. The follicle cells in the ovary of *Propylea japonica* played a crucial role in the formation of the vitelline membrane and eggshell, as they facilitated the transport of vitellogenin from [27]. These follicle cell layers were established early during oocyte development and served a protective function [28,29].

The state of the uterus underwent changes during egg development: it contracted and became inconspicuous in the absence of eggs but expanded and compressed the uterine epithelium when eggs were present. The vagina was connected to the uterus, and once the eggs were fully developed, the genital plate opened for egg deposition. However, these reproductive structures differed from Di Palma's descriptions for *Dermanyssina* [30].

In females, the ovaries contained oocytes at four developmental stages regardless of mating status. The morphological structure of oocytes was similar under different mating conditions, and the morphology matched Di Palma's descriptions [7]. Oocytes in females underwent all four stages of development before and after mating, indicating that they must reach a specific level to become sperm-receptive. Moreover, oocyte development in females was regulated by the female itself and remained unaffected by mating. Early-maturing oocytes were fertilized, developed into eggs, and migrated to the uterus, which might explain why mating status had no impact. Consequently, this balance within the ovary ensured readiness for fertilization. If mature oocytes in unmated females remained unfertilized, they might either undergo apoptosis or be reabsorbed. Zhao's study on *Phenacoccus solenopsis* Tinsley found no significant morphological differences in the ovaries between the mated and unmated females [31]. In mated females, oocytes absorb nutrients from surrounding nurse cells to develop into embryos and complete reproduction, whereas, in unmated females, unfertilized oocytes might either be reabsorbed or fail to develop further. Apoptosis during oogenesis aided insects in maintaining reproductive efficiency under unfavorable conditions [32,33], while in fruit flies, apoptosis checkpoints ensured proper cell development [32].

The mechanisms underlying the occurrence of position shifts during egg development and the establishment of positional relationships between the first and second eggs remained elusive. It had been noted that the synthesis and secretion of the eggshell were facilitated by uterine glands [7]. Our observations showed that 10 h after mating, the first egg had four centrally positioned cells. Toyoshima described that 10 h after mating, two nuclei appeared in the egg and fused by 12.7 h, and combined pronuclei were visible by 13.5 h [13]. However, our observations revealed some temporal discrepancies to Toyoshima's findings. Specifically, we observed two cellular structures at the center of the first egg 9 h after mating, indicating imminent sperm-egg fusion. By 10 h post-mating, the presence of four cells within the egg suggested successful fertilization and cell division occurring. Consequently, we estimated that fusion occurs between 9 and 10 h post-mating, which was earlier than Toyoshima's estimated timeframe of 13.5 h. Our study demonstrated that, at this time point, there were already two cells present within the egg, implying that both fusion and cell division had commenced prior to Toyoshima's proposed timeline for embryonic development initiation. These variations might potentially arise from differences in rearing conditions, as well as individual variability. In summary, we investigated the morphological characteristics of various reproductive structures in female mites and examined their alterations under different mating conditions. Firstly, all reproductive structures were observable within the female mite's body following mating. However, under unmated conditions, apart from the lyrate organ and ovaries, other reproductive structures were scarcely detectable through electron microscopy. Secondly, only the nucleus of the lyrate organ was affected by mating without any impact on the morphology of other reproductive structures. Finally, no significant changes in the morphology of these reproductive structures were observed at

different time points after mating. The morphology and structure of oocytes in the ovaries of females remained similar after mating, exhibiting no significant differences compared to those in the unmated state. The development of the egg occurs within 0 to 16 h post-mating, encompassing four stages: nutrient accumulation (4–9 h), relocation of the egg (around 10 h), formation of the eggshell (12–13 h), and early embryogenesis, leading to oviposition (14–16 h). Embryonic development occurred at 9 h post-mating, while two cells could be seen in the first egg, analogous to the union of sperm and egg cells. Then, 10 h post-mating, the first egg in the uterus showed four cells at its center, suggesting early cleavage divisions. Sperm and egg fusion should occur between 9 and 10 h. By 13 h, the second egg contained a single cell. These could potentially be fused sperm cells derived from the second egg.

Author Contributions: Conceptualization, B.H. and M.L.; methodology, X.J.; validation, Y.H. and X.X.; formal analysis, B.H.; investigation, M.L.; data curation, B.H., M.L. and X.J.; writing—original draft preparation, B.H. and M.L.; writing—review and editing, B.H. and M.L.; supervision, Y.H.; project administration, X.X.; funding acquisition, B.Z. and X.X. All authors have read and agreed to the published version of the manuscript.

Funding: This work was supported by National Key R&D Program of China (2023YFD1400600).

Institutional Review Board Statement: Not applicable.

Data Availability Statement: The raw data supporting the conclusions of this article will be made available by the authors upon request.

Conflicts of Interest: The authors declare no conflicts of interest.

References

1. Van Lenteren, J.C. The state of commercial augmentative biological control: Plenty of natural enemies, but a frustrating lack of uptake. *BioControl* **2012**, *57*, 1–20. [[CrossRef](#)]
2. Helle, W.; Sabelis, M.W. Spider mites, their biology, natural enemies and control. *Exp. Appl. Acarol.* **1986**, *2*, 277–281.
3. Sabelis, M.W.; Harmsen, R. Special Issue Population dynamics of plant-inhabiting mites. *Exp. Appl. Acarol.* **1992**, *14*, ii. [[CrossRef](#)]
4. Sabelis, M.W.; Janssen, A. Evolution of Life-History Patterns in the Phytoseiidae. In *Mites*; Houck, M.A., Ed.; Springer: Boston, MA, USA, 1994; pp. 70–98.
5. Alberti, G. Genital system of Gamasida and its bearing on phylogeny. In *Progress in Acarology*; ChannaBasavanna, G.P., Virakmath, C.A., Eds.; Oxford & IBH Publishing: New Delhi, India, 1988; Volume 1, pp. 197–204.
6. Nuzzaci, G.; Di Palma, A.; Aldini, P. Functional morphology of the female genital system in *Typhlodromus* spp. (Acari: Phytoseiidae). In *Acarology: Proceedings of the 10th International Congress*; Walter, D.E., Proctor, H., Norton, R.A., Colloff, M., Halliday, R.B., Eds.; CSIRO Publishing: Melbourne, Australia, 2001; pp. 196–202.
7. Di Palma, A.; Alberti, G. Fine structure of the female genital system in phytoseiid mites with remarks on egg nutritive development, sperm-access system, sperm transfer, and capacitation (Acari, Gamasida, Phytoseiidae). *Exp. Appl. Acarol.* **2001**, *25*, 525–591. [[CrossRef](#)] [[PubMed](#)]
8. Evans, G.O.; Till, W.M. Mesostigmatic mites of Britain and Ireland (Chelicerata: Acari-Parasitiformes): An introduction to their external morphology and classification. *Trans. Zool. Soc. Lond.* **1979**, *35*, 139–262. [[CrossRef](#)]
9. Helle, W.; Bolland, H.R.; Van Arendonk, R.; De Boer, R.; Schulten, G.G.M.; Russell, V.M. Genetic evidence for biparental males in haplo-diploid predator mites (Acarina: Phytoseiidae). *Genetica* **1978**, *49*, 165–171. [[CrossRef](#)]
10. Hoy, M.A. Parahaploidy of the “arrhenotokous” predator, *Metaseiulus occidentalis* (Acarina: Phytoseiidae), demonstrated by x-irradiation of males. *Entomol. Exp. Appl.* **1979**, *26*, 97–104. [[CrossRef](#)]
11. Hoy, M.A. Genetics and genetic improvement of the Phytoseiidae. *Ann. Rev. Entomol.* **1985**, *30*, 345–370. [[CrossRef](#)]
12. Zhang, B. Reproductive Mechanism of *Phytoseiulus persimilis* by Gamma Irradiation. Master’s Thesis, Graduate School of Chinese Academy of Agricultural Sciences, Beijing, China, 2016.
13. Toyoshima, S.; Nakamura, M.; Nagahama, Y.; Amano, H. Process of Egg Formation in the Female Body Cavity and Fertilization in Male Eggs of *Phytoseiulus Persimilis* (Acari: Phytoseiidae). *Exp. Appl. Acarol.* **2000**, *24*, 441–451. [[CrossRef](#)]
14. Yan, H.; Wang, E. Both host and diet shape bacterial communities of predatory mites. *Insect Sci.* **2024**, *31*, 551–561. [[CrossRef](#)]
15. Li, M. Study on the Reproductive Process and Reproductive Related Gene of *Phytoseiulus persimilis*. Master’s Thesis, Graduate School of Chinese Academy of Agricultural Sciences, Beijing, China, 2023.
16. Su, Y. The Study on Chemosensory Function of Three Phytoseiid Mites in the Process of Prey Recognition. Master’s Thesis, Graduate School of Chinese Academy of Agricultural Sciences, Beijing, China, 2021.
17. Jiang, X. Reproductive and Sperm Transfer Structures of *Phytoseiulus persimilis*. Doctoral Thesis, Graduate School of Chinese Academy of Agricultural Sciences, Beijing, China, 2019.

18. Michael, A.D. On the variations in the internal anatomy of the Gamasina especially in that of the genital organs, and their mode of coition. *Trans. Linn. Soc. Lond.* **1892**, *5*, 281–317. [[CrossRef](#)]
19. Alberti, G.; Hänel, H. Fine structure of the genital system in the bee parasite, *Varroa jacobsoni* (Gamasida: Dermanyssina) with remarks on spermiogenesis, spermatozoa and capacitation. *Exp. Appl. Acarol.* **1986**, *2*, 63–104. [[CrossRef](#)]
20. Wei, H.; Geng, T.; Wu, H.; Lou, D.; Wu, C.; Xie, Y.; Lu, F.; Wang, C. Morphological characteristics of inner reproductive system of *Microcephalus sangensis* and its changes in different developmental stages. *J. Trop. Crops* **2023**, *44*, 1023–1029.
21. Xiao, P.; Ma, Y.; Li, H.; Han, Q. Morphological changes of inner reproductive system of Psyllid in Asian citrus. *Chin. J. Environ. Entomol.* **2017**, *39*, 1207–1213.
22. Amano, H.; Chant, D.A. Mating behaviour and reproductive mechanisms of two species of predacious mites, *Phytoseiulus persimilis* Athias-Henriot and *Amblyseius andersoni* (Chant) (Acarina: Phytoseiidae). *Acarologia* **1979**, *20*, 196–213.
23. Schulten, G.G.; Pseudoarrhenotoky, M. *Spider Mites, Their Biology, Natural Enemies and Control*; Helle, W., Sabelis, M.W., Eds.; Elsevier: Amsterdam, The Netherlands, 1985; Volume 1B, pp. 67–71.
24. Dosse, G. Über den Kopulationsvorgang bei Raubmilben aus der Gattung *Typhlodromus* (Acari, Phytoseiidae). *Pflanzenschutzberichte* **1959**, *22*, 125–133.
25. Alberti, G.; Coons, L.B. Acari—Mites. In *Microscopic Anatomy of Invertebrates*; Harrison, F.W., Ed.; Wiley-Liss: New York, NY, USA, 1999; Volume 8, pp. 515–1265.
26. Gustafsson, J.K.; Johansson, M.E.V. The role of goblet cells and mucus in intestinal homeostasis. *Nat. Rev. Gastroenterol. Hepatol.* **2022**, *19*, 785–803. [[CrossRef](#)]
27. Zhang, T.; Li, K.; Zhang, L.; Wang, B. Histological study of ovulation in *Propylea japonica* (Thunberg). *J. Northwest A & F Univ.* **2009**, *37*, 175–180.
28. Kelly, T.J.; Telfer, W.H. The function of the follicular epithelium in vitellogenic *Oncopeltus follicles*. *Tissue Cell* **1979**, *114*, 663–672. [[CrossRef](#)]
29. Nan, G. Study on the Relationship between Oocyte Entry and Oocyte Uptake of Vitelline Proteinogen by Brown Planthopper Yeast Symbiotic Bacteria. Master's Thesis, China Jiliang University, Hangzhou, China, 2016.
30. Di Palma, A.; Seeman, O.D.; Alberti, G. Complexity, adaptations and variations in the secondary insemination system of female Dermanyssina mites (Acari: Anactinothrichida: Gamasida): The case of *Afrocypholaelaps africana*. *Exp. Appl. Acarol.* **2017**, *72*, 191–203. [[CrossRef](#)]
31. Zhao, C. Effects of Mating Behavior and Symbiotic Bacteria on Preembryonic Development of *Planococcus fusococcus*. Master's Thesis, Zhejiang Normal University, Jinhua, China, 2016.
32. Peterson, J.S.; Timmons, A.K.; Mondragon, A.A.; McCall, K. The End of the Beginning: Cell Death in the Germline. *Curr. Top. Dev. Biol.* **2015**, *114*, 93–119. [[PubMed](#)]
33. Nezis, I.P.; Stravopodis, D.J.; Papassideri, I.; Robert-Nicoud, M.; Margaritis, L.H. Stage-specific apoptotic patterns during *Drosophila* oogenesis. *Eur. J. Cell Biol.* **2000**, *79*, 610–620. [[CrossRef](#)] [[PubMed](#)]

Disclaimer/Publisher's Note: The statements, opinions and data contained in all publications are solely those of the individual author(s) and contributor(s) and not of MDPI and/or the editor(s). MDPI and/or the editor(s) disclaim responsibility for any injury to people or property resulting from any ideas, methods, instructions or products referred to in the content.